1236 *Organometallics* **2011,** *30,* 1236–1252
DOI: 10.1021/om101152m

ORGANOMETALLICS
Article

Mechanistic Investigation of the Hydrogenation of Ketones Catalyzed by a Ruthenium(II) Complex Featuring an N-Heterocyclic Carbene with a Tethered Primary Amine Donor: Evidence for an Inner Sphere Mechanism

Wylie W. N. O, Alan J. Lough, and Robert H. Morris*

Davenport Laboratory, Department of Chemistry, University of Toronto, 80 St. George Street, Toronto, Ontario M5S 3H6, Canada

Received December 7, 2010

The complex [Ru(*p*-cymene)(*m*-CH_2NH_2)Cl]PF_6 (**1**) catalyzes the H_2-hydrogenation of ketones in basic THF under 25 bar of H_2 at 50 °C with a turnover frequency (TOF) of up to 461 h^{-1} and a maximum conversion of 99%. When the substrate is acetophenone, the TOF decreases significantly as the catalyst to substrate ratio is increased. The rate law was then determined to be rate = $k_H[Ru]_{tot}[H_2]/(1 + K_{eq}[ketone])$, and [**1**] is equal to $[Ru]_{tot}$ if catalyst decomposition does not occur. This is consistent with the heterolytic splitting of dihydrogen at the active ruthenium species as the rate-determining step. In competition with this reaction is the reversible addition of acetophenone to the active species to give an enolate complex. The transfer to the ketone of a hydride and proton equivalent that are produced in the heterolytic splitting reaction yields the product in a fast, low activation barrier step. The kinetic isotope effect was measured using D_2 gas and acetophenone-d_3, and this gave values (k_H/k_D) of 1.33 ± 0.15 and 1.29 ± 0.15, respectively. The ruthenium hydride complex [Ru(*p*-cymene)(*m*-CH_2NH_2)H]PF_6 (**2**) was prepared, as this was postulated to be a crucial intermediate in the outer-sphere bifunctional mechanism. This is inactive under catalytic conditions unless it is activated by a base. DFT computations suggest that the energy barriers for the addition of dihydrogen, heterolytic splitting of dihydrogen, and concerted transfer of H^+/H^- to the ketone for the outer-sphere mechanism would be respectively 18.0, 0.2, and 33.5 kcal/mol uphill at 298 K and 1 atm. On the other hand, the energy barriers for an inner-sphere mechanism involving the decoordination of the amine group of the NHC ligand, the heterolytic splitting of dihydrogen across a Ru−O(alkoxide) bond, and hydride migration to the coordinated ketone, are respectively 15.5, 17.5, and 15.6 kcal/mol uphill at 298 K and 1 atm. This is more consistent with the experimental observation that the heterolytic splitting of dihydrogen is the turnover-limiting step. This was confirmed by showing that an analogous complex with a tethered teritiary amine group has comparable activity for the H_2-hydrogenation of acetophenone. The related complex [Os(*p*-cymene)(*m*-CH_2NH_2)Cl]PF_6 (**6**) was synthesized by a transmetalation reaction with [Ni(*m*-CH_2NH_2)$_2$]$(PF_6)_2$ (**5**) and [Os(*p*-cymene)Cl_2]$_2$, and its catalytic activity toward hydrogenation of acetophenone was also investigated.

Introduction

The hydrogenation of polar bonds using molecular hydrogen has remained by far the most efficient process in terms of atom economy.[1,2] However, dihydrogen is inert to reaction with most organic substrates of interest, and so it must be activated by a transition-metal complex, forming metal hydride complexes,[3] or more recently by main-group compounds such as frustrated Lewis pairs.[4] Bifunctional catalysis,[5,6] which was originally proposed by Noyori and co-workers in the pioneering work in the hydrogenation of polar bonds using the catalyst RuH(η^6-*p*-cymene)((*S,S*)-Tsdpen) (Tsdpen = *N*-(*p*-toluenesulfonyl)-1,2-diphenylethylenediamine)[7] and, more generally, late-transition-metal catalysts containing M−H and N−H groups[8,9] have superior

*To whom correspondence should be addressed. E-mail: rmorris@chem.utoronto.ca.

(1) (a) Kubas, G. J. *Chem. Rev.* **2007**, *107*, 4152–4205. (b) de Vries, J. G., Elsevier, C. J., Eds. *The Handbook of Homogeneous Hydrogenation*; Wiley-VCH: Weinheim, Germany, 2004; Vols. *1*−*3*.

(2) Ito, M.; Ikariya, T. *Chem. Commun.* **2007**, 5134–5142.

(3) (a) Jessop, P. G.; Morris, R. H. *Coord. Chem. Rev.* **1992**, *121*, 155–284. (b) Morris, R. H. *Can. J. Chem.* **1996**, *74*, 1907–1915. (c) Rosales, M. *Coord. Chem. Rev.* **2000**, *196*, 249–280. (d) Young, M. B.; Barrow, J. C.; Glass, K. L.; Lundell, G. F.; Newton, C. L.; Pellicore, J. M.; Rittle, K. E.; Selnick, H. G.; Stauffer, K. J.; Vacca, J. P.; Williams, P. D.; Bohn, D.; Clayton, F. C.; Cook, J. J.; Krueger, J. A.; Kuo, L. C.; Lewis, S. D.; Lucas, B. J.; McMasters, D. R.; Miller-Stein, C.; Pietrak, B. L.; Wallace, A. A.; White, R. B.; Wong, B.; Yan, Y.; Nantermet, P. G. *J. Med. Chem.* **2004**, *47*, 2995–3008. (e) DuBois, M. R.; DuBois, D. L. *Chem. Soc. Rev.* **2009**, *38*, 62–72.

(4) Stephan, D. W.; Erker, G. *Angew. Chem., Int. Ed.* **2010**, *49*, 46–76.

(5) (a) Muniz, K. *Angew. Chem., Int. Ed.* **2005**, *44*, 6622–6627. (b) Ito, M.; Ikariya, T. *J. Synth. Org. Chem. Jpn.* **2008**, *66*, 1042–1048. (c) Grützmacher, H. *Angew. Chem., Int. Ed.* **2008**, *47*, 1814–1818. (d) Kuwata, S.; Ikariya, T. *Dalton Trans.* **2010**, *39*, 2984–2992. (e) Grotjahn, D. B. *Top. Catal.* **2010**, *53*, 1009–1014.

(6) Ikariya, T.; Murata, K.; Noyori, R. *Org. Biomol. Chem.* **2006**, *4*, 393–406.

(7) Haack, K. J.; Hashiguchi, S.; Fujii, A.; Ikariya, T.; Noyori, R. *Angew. Chem., Int. Ed.* **1997**, *36*, 285–288.

(8) Noyori, R.; Yamakawa, M.; Hashiguchi, S. *J. Org. Chem.* **2001**, *66*, 7931–7944.

(9) Clapham, S. E.; Hadzovic, A.; Morris, R. H. *Coord. Chem. Rev.* **2004**, *248*, 2201–2237.

 Published on Web 02/22/2011

activities in the selective reduction of polar bonds to produce valuable alcohols and amines. Several studies, both theoretical[10−12] and experimental,[13−15] including the study of kinetic isotope effects,[16−18] have been conducted to understand the mechanism of action using the "NH-effect" and the bifunctional nature of the true form of catalytically active species. The presence of the N−H group and its relationship to the outer-sphere bifunctional[19,20] and inner-sphere mechanisms[21,22] have also been studied by many research groups.

The many catalyst systems that were studied by our research group[23−28] which undergo efficient H_2-hydrogenation of ketones and imines, including those of *trans*-$Ru(H)_2$((*R*)-binap)(tmen), (*OC*-6-22)-$Ru(H)_2(PPh_3)_2$(tmen) (tmen = 2,3-dimethylbutane-2,3-diamine), and *trans*-$Ru(H)_2(\kappa^4\text{-}P_2(NH)_2)$[26,29] ($P_2(NH)_2$ = tetradentate diphosphinediamine ligand), were found to have the heterolytic splitting of the coordinated η^2-H_2 ligand on the active species as the rate-determining step from various mechanistic and computational studies.[25−28] These are active catalysts, without prior activation with base, and catalyze efficiently the reduction of ketones by H_2 under mild conditions.[24−27] The energy barrier calculated for the model complex (*OC*-6-22)-$Ru(H)_2(PH_3)_2$(en) (en = ethylenediamine) was found to be higher in the heterolytic splitting of H_2 compared to the concerted transfer of H^+/H^- to the ketone in a six-membered-ring transition state.[8−11] The corresponding coordinatively unsaturated complexes containing a ruthenium−amido bond were isolated, and these were also found to activate dihydrogen to give the *trans*-dihydride complexes.[24−27] For the system *trans*-$Ru(H)_2$(diamine)((*R*)-binap), Bergens and coworkers suggested a ruthenium(II) alkoxide complex was indeed formed prior to the formation of such amido complexes.[15,30]

Not much work has been devoted to study the mechanism of action of catalysts containing phosphine−amine ligands (P−NH_2).[31−34] The ruthenium catalysts containing these ligands effect not only the reduction of ketones[32] but also the hydrogenation of a broad range of substrates, including imines,[34] esters,[35] epoxides,[31] and other polar bonds.[36] All these may utilize the same bifunctional mechanism involving the action of the M−H and N−H groups. The notion of replacing the phosphine with an N-heterocyclic carbene (NHC) donor, in particular, a donor-functionalized NHC, is therefore attractive to achieve the goal of greener chemistry.[37] We have previously reported that the transfer hydrogenation catalyst [Ru(*p*-cymene)(*m*-CH_2NH_2)Cl]PF_6 (**1**) is effective for the hydrogenation of acetophenone to 1-phenylethanol in basic 2-propanol at 75 °C. This system reached a maximum conversion of 96% and a turnover frequency (TOF) of 880 h^{-1} (Figure 1).[38] Here we present our study toward its H_2-hydrogenation activity in the reduction of ketones and a detailed mechanistic investigation, including kinetic studies and theoretical computations that were performed to study the possibility of the cooperative nature of the ligand and the metal center in this new class of ligand system.

(10) Yamakawa, M.; Ito, H.; Noyori, R. *J. Am. Chem. Soc.* **2000**, *122*, 1466–1478.

(11) (a) Di Tommaso, D.; French, S. A.; Catlow, C. R. A. *J. Mol. Struct.* (*THEOCHEM*) **2007**, *812*, 39–49. (b) Puchta, R.; Dahlenburg, L.; Clark, T. *Chem. Eur. J.* **2008**, *14*, 8898–8903. (c) Chen, Y.; Tang, Y. H.; Lei, M. *Dalton Trans.* **2009**, 2359–2364. (d) Lei, M.; Zhang, W. C.; Chen, Y.; Tang, Y. H. *Organometallics* **2010**, *29*, 543–548.

(12) (a) Zhang, H. H.; Chen, D. Z.; Zhang, Y. H.; Zhang, G. Q.; Liu, J. B. *Dalton Trans.* **2010**, *39*, 1972–1978. (b) Chen, Z.; Chen, Y.; Tang, Y. H.; Lei, M. *Dalton Trans.* **2010**, *39*, 2036–2043.

(13) (a) Maire, P.; Buttner, T.; Breher, F.; Le Floch, P.; Grutzmacher, H. *Angew. Chem., Int. Ed.* **2005**, *44*, 6318–6323. (b) Friedrich, A.; Drees, M.; auf der Gunne, J. S.; Schneider, S. *J. Am. Chem. Soc.* **2009**, *131*, 17552–17553.

(14) (a) Sandoval, C. A.; Ohkuma, T.; Utsumi, N.; Tsutsumi, K.; Murata, K.; Noyori, R. *Chem. Asian J.* **2006**, *1*, 102–110. (b) Ohkuma, T.; Utsumi, N.; Tsutsumi, K.; Murata, K.; Sandoval, C.; Noyori, R. *J. Am. Chem. Soc.* **2006**, *128*, 8724–8725.

(15) Hamilton, R. J.; Leong, C. G.; Bigam, G.; Miskolzie, M.; Bergens, S. H. *J. Am. Chem. Soc.* **2005**, *127*, 4152–4153.

(16) Sandoval, C. A.; Ohkuma, T.; Muniz, K.; Noyori, R. *J. Am. Chem. Soc.* **2003**, *125*, 13490–13503.

(17) Kass, M.; Friedrich, A.; Drees, M.; Schneider, S. *Angew. Chem., Int. Ed.* **2009**, *48*, 905–907.

(18) Zimmer-De Iuliis, M.; Morris, R. H. *J. Am. Chem. Soc.* **2009**, *131*, 11263–11269.

(19) (a) Noyori, R.; Ohkuma, T. *Angew. Chem., Int. Ed.* **2001**, *40*, 40–73. (b) Ma, G. B.; McDonald, R.; Ferguson, M.; Cavell, R. G.; Patrick, B. O.; James, B. R.; Hu, T. Q. *Organometallics* **2007**, *26*, 846–854. (c) Baratta, W.; Ballico, M.; Esposito, G.; Rigo, P. *Chem. Eur. J.* **2008**, *14*, 5588–5595. (d) Sandoval, C. A.; Shi, Q. X.; Liu, S. S.; Noyori, R. *Chem. Asian J.* **2009**, *4*, 1221–1224.

(20) Ito, M.; Hirakawa, M.; Murata, K.; Ikariya, T. *Organometallics* **2001**, *20*, 379–381.

(21) (a) Leong, C. G.; Akotsi, O. M.; Ferguson, M. J.; Bergens, S. H. *Chem. Commun.* **2003**, 750–751. (b) Phillips, S. D.; Fuentes, J. A.; Clarke, M. L. *Chem. Eur. J.* **2010**, *16*, 8002–8005.

(22) Lundgren, R. J.; Rankin, M. A.; McDonald, R.; Schatte, G.; Stradiotto, M. *Angew. Chem., Int. Ed.* **2007**, *46*, 4732–4735.

(23) Abdur-Rashid, K.; Lough, A. J.; Morris, R. H. *Organometallics* **2001**, *20*, 1047–1049.

(24) Abdur-Rashid, K.; Faatz, M.; Lough, A. J.; Morris, R. H. *J. Am. Chem. Soc.* **2001**, *123*, 7473–7474.

(25) (a) Abdur-Rashid, K.; Clapham, S. E.; Hadzovic, A.; Harvey, J. N.; Lough, A. J.; Morris, R. H. *J. Am. Chem. Soc.* **2002**, *124*, 15104–15118. (b) Abbel, R.; Abdur-Rashid, K.; Faatz, M.; Hadzovic, A.; Lough, A. J.; Morris, R. H. *J. Am. Chem. Soc.* **2005**, *127*, 1870–1882.

(26) Rautenstrauch, V.; Hoang-Cong, X.; Churlaud, R.; Abdur-Rashid, K.; Morris, R. H. *Chem. Eur. J.* **2003**, *9*, 4954–4967.

(27) Clapham, S. E.; Morris, R. H. *Organometallics* **2005**, *24*, 479–481.

(28) Hadzovic, A.; Song, D.; MacLaughlin, C. M.; Morris, R. H. *Organometallics* **2007**, *26*, 5987–5999.

(29) (a) Li, T.; Churlaud, R.; Lough, A. J.; Abdur-Rashid, K.; Morris, R. H. *Organometallics* **2004**, *23*, 6239–6247. (b) Li, T.; Bergner, I.; Haque, F. N.; Zimmer-De Iuliis, M.; Song, D.; Morris, R. H. *Organometallics* **2007**, *26*, 5940–5949.

(30) Hamilton, R. J.; Bergens, S. H. *J. Am. Chem. Soc.* **2008**, *130*, 11979–11987.

(31) Ito, M.; Hirakawa, M.; Osaku, A.; Ikariya, T. *Organometallics* **2003**, *22*, 4190–4192.

(32) (a) Guo, R.; Lough, A. J.; Morris, R. H.; Song, D. *Organometallics* **2004**, *23*, 5524–5529. (b) Jia, W. L.; Chen, X. H.; Guo, R. W.; Sui-Seng, C.; Amoroso, D.; Lough, A. J.; Abdur-Rashid, K. *Dalton Trans.* **2009**, 8301–8307.

(33) (a) Dahlenburg, L.; Gotz, R. *Eur. J. Inorg. Chem.* **2004**, 888–905. (b) Blaquiere, N.; Diallo-Garcia, S.; Gorelsky, S. I.; Black, D. A.; Fagnou, K. *J. Am. Chem. Soc.* **2008**, *130*, 14034–14035.

(34) Abdur-Rashid, K.; Guo, R. W.; Lough, A. J.; Morris, R. H.; Song, D. T. *Adv. Synth. Catal.* **2005**, *347*, 571–579.

(35) (a) Saudan, L. A.; Saudan, C. M.; Debieux, C.; Wyss, P. *Angew. Chem., Int. Ed.* **2007**, *46*, 7473–7476. (b) Kuriyama, W.; Ino, Y.; Ogata, O.; Sayo, N.; Saito, T. *Adv. Synth. Catal.* **2010**, *352*, 92–96.

(36) (a) Ito, M.; Sakaguchi, A.; Kobayashi, C.; Ikariya, T. *J. Am. Chem. Soc.* **2007**, *129*, 290–291. (b) Ito, M.; Koo, L. W.; Himizu, A.; Kobayashi, C.; Sakaguchi, A.; Ikariya, T. *Angew. Chem., Int. Ed.* **2009**, *48*, 1324–1327.

(37) (a) Lee, H. M.; Lee, C. C.; Cheng, P. Y. *Curr. Org. Chem.* **2007**, *11*, 1491–1524. (b) Kuhl, O. *Chem. Soc. Rev.* **2007**, *36*, 592–607. (c) Normand, A. T.; Cavell, K. J. *Eur. J. Inorg. Chem.* **2008**, 2781–2800. (d) Corberan, R.; Mas-Marza, E.; Peris, E. *Eur. J. Inorg. Chem.* **2009**, 1700–1716. (d) Diez-Gonzalez, S.; Marion, N.; Nolan, S. P. *Chem. Rev.* **2009**, *109*, 3612–3676.

(38) O, W. W. N.; Lough, A. J.; Morris, R. H. *Organometallics* **2009**, *28*, 6755–6761.

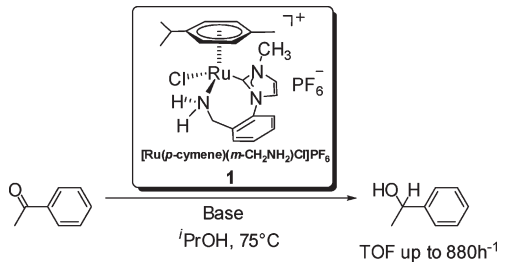

Figure 1. Transfer hydrogenation of acetophenone catalyzed by complex **1** in basic 2-propanol.

Table 1. H_2-Hydrogenation of Acetophenone to 1-Phenylethanol Catalyzed by Complex 1

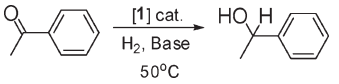

entry[a]	C/B/S[b]	solvent	base	conversn[c] (%/h)		TOF (h^{-1})[d]
1	1/8/200	^{i}PrOH	KO^{t}Bu	96/1	99/1.5	287
2	1/8/200	THF	KO^{t}Bu	88/1	99/2	213
3	1/8/200	THF	NaO^{t}Bu	5/1	11/2	
4	1/0/200	THF	none	0/1		
5	0/8/200	THF	KO^{t}Bu	0/1		
6	1/8/600	THF	KO^{t}Bu	20/1	57/2.5	122
7	1/8/1200	THF	KO^{t}Bu	6/1	28/3	73
8[e]	1/8/200	THF	KO^{t}Bu	0/1		

[a] Reactions were carried out in a 50 mL Parr hydrogenation reactor at 25 bar of H_2 pressure at 50 °C using THF or ^{i}PrOH (6 mL) as the solvent. [b] C/B/S = catalyst/base/substrate. [c] Conversions were determined by GC and are reported as an average of two runs. [d] TOF = turnover frequency, measured from the slope of the linear portion of an [alcohol] versus time plot. [e] Reaction conducted under argon.

Results and Discussion

H_2-Hydrogenation of Acetophenone Catalyzed by Complex 1. The results pertaining to the catalytic activity of complex **1** in the H_2-hydrogenation of acetophenone are given in Table 1. Full conversion to 1-phenylethanol is achieved in 1.5 h under 25 bar of H_2 in 2-propanol at 50 °C with a catalyst to base to substrate (C/B/S) ratio of 1/8/200 on activation in the presence of potassium *tert*-butoxide (KO^{t}Bu) as the base. This took somewhat longer (2 h) when an aprotic solvent, tetrahydrofuran (THF), was used instead (Table 1, entries 1 and 2). The ruthenium(II) complex is not a catalyst when not activated by base. It exhibited low activity when sodium *tert*-butoxide, which has a low solubility in THF, was used. In addition, the ruthenium(II) complex is not a catalyst when activated by base in the absence of H_2 in THF (Table 1, entries 3, 4 and 8). More importantly, an increase in substrate loading to a catalyst to substrate (C/S) ratio of 1/1200 decreased the TOF value by 3-fold, giving a value of 73 h^{-1} (Table 1, entries 6 and 7). The catalyst [Ru(η^5-Cp*)(*m*-CH_2NH_2)(py)]PF_6 (Cp* = pentamethylcyclopentadienyl; py = pyridine), which contains the same chelating primary amine−NHC ligand, tolerates high substrate loading (C/S ratio up to 1/11 500) when activated by base.[39]

(39) O, W. W. N.; Lough, A. J.; Morris, R. H. *Chem. Commun.* **2010**, *46*, 8240–8242.

Table 2. H_2-Hydrogenation of Ketones Catalyzed by Complex 1

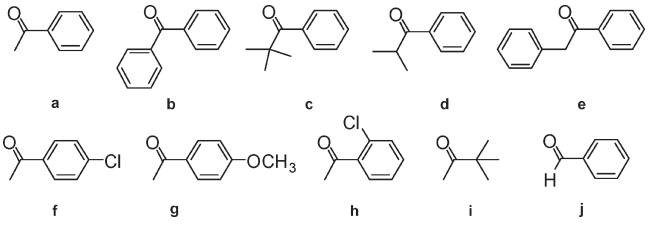

entry[a]	substrate	conversn[c] (%/h)		TOF (h^{-1})
1	**a**	88/1	99/2	213
2	**b**	78/1	98/2	208
3[b]	**b**	40/1	77/3	179
4	**c**	94/1	99/1.5	461
5	**d**	94/1	99/1.5	377
6	**e**	0/1	0/2	
7	**f**	94/1	99/1.5	260
8	**g**	79/1	96/2.5	215
9	**h**	3/1	4/1.5	5
10	**i**	74/1	99/2.5	164
11	**j**	70/0.16	99/0.5	838

[a] Reactions were carried out in a 50 mL Parr hydrogenation reactor at 25 bar of H_2 pressure at 50 °C using THF (6 mL). Potassium *tert*-butoxide was used as base. The C/B/S ratio was 1/8/200. [b] The C/B/S ratio was 1/8/400. [c] Conversions were determined by GC and are reported as an average of two runs.

H_2-Hydrogenation of Other Ketones Catalyzed by Complex 1. Other ketones with different steric bulk were investigated (Table 2, entries 1−6). In general, TOF values increase with a larger group next to the polar bond. Of note, substrates without α-C−H protons next to the carbonyl group did not show inhibition of the catalysis by the substrate. For example, a 2-fold increase in the substrate loading in the hydrogenation of benzophenone gave similar initial rates and TOF values (Table 2, entries 4 and 5, and the Supporting Information, Figure S1). On the other hand, complex **1** did not catalyze the hydrogenation of deoxybenzoin in basic THF (entry 6). All these results are suggestive of the formation of an enolate complex derived from the active ruthenium species. This likely causes a decrease in the concentration of the active ruthenium species within the catalytic cycle (vide infra). An increase in the donor ability on going from chloro to methoxy substituents at the 4′-position of the aryl group on the ketone led to a slight decrease in the TOF values (entries 7 and 8). Placing the chloro group ortho to the ketone results in a dramatic decrease in rate (entry 9). Pinacolone and benzaldehyde were also effectively hydrogenated under similar reaction conditions (Table 2, entries 10 and 11).

Kinetic Studies. The mechanism of action of the H_2-hydrogenation of ketones catalyzed by complex **1** was probed by determining the rate law. Acetophenone was chosen as the substrate of interest, and its concentration along with that of 1-phenylethanol was conveniently monitored by gas chromatography (GC). The catalytic conditions were varied from the standard conditions (0.83 mM [**1**], 25 bar of H_2, 0.17 M acetophenone and 7.4 mM potassium *tert*-butoxide; catalyst/base/H_2/ketone = 1/8/120/200) by changing the concentration of a single component of interest, using 0.28−0.83 mM of **1**, 5−25 bar of H_2, 0.17−1.0 M

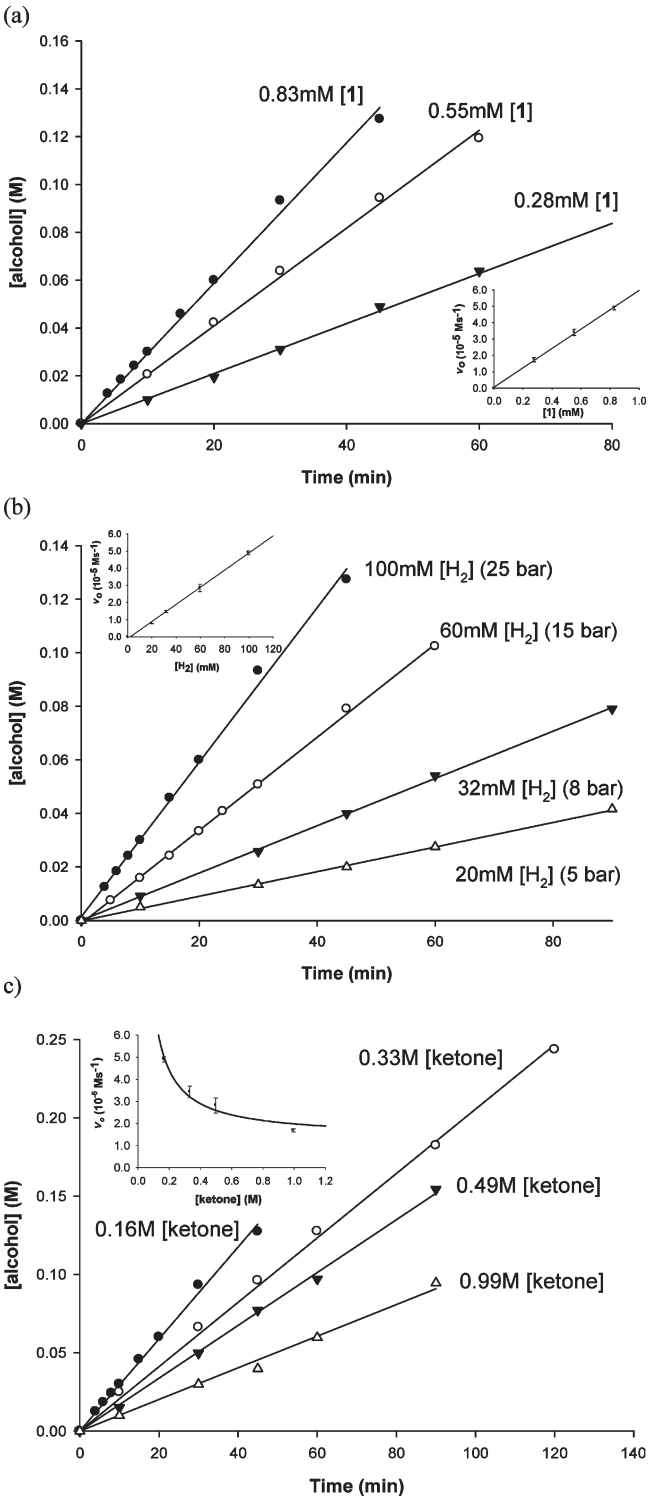

Figure 2. Kinetic data showing the production of 1-phenylethanol from acetophenone catalyzed by complex **1** in basic THF: (a) dependence on the catalyst concentration (**1**); (b) dependence on the hydrogen concentration; (c) dependence on the acetophenone concentration. The inset shows the dependence of initial rates (v_0, $\times 10^{-5}$ M s^{-1}) and the concentration of the analyte of interest. Details of the reaction conditions are given in Table 3 and in the Supporting Information (Tables S1−S3).

acetophenone, 0−35 mM 1-phenylethanol, and 2.9−18 mM potassium *tert*-butoxide. The reaction temperature was kept at 50 °C for all of the runs. Some representative catalytic conditions and kinetic data from the initial linear portion of the plots of [alcohol] versus time are given in Figure 2 and in Table 3.

Table 3. Kinetic Data for the Hydrogenation of Acetophenone Catalyzed by Complex 1

				initial rate (v_0), 10^{-5} M s^{-1}	
run[a]	[**1**], mM	$[H_2/D_2]^b$, mM	[ketone], M	exptl[c]	calcd[d]
1	0.28	100	0.17	1.7	1.6
2	0.55	100	0.17	3.4	3.2
3	0.83	100	0.17	4.9	4.8
4	0.83	60	0.17	2.9	2.9
5	0.83	32	0.17	1.5	1.5
6	0.83	20	0.17	0.76	0.97
7	0.83	100	0.33	3.4	3.6
8	0.83	100	0.50	2.8	2.8
9	0.83	100	1.0	1.7	1.7
10[e]	0.83	33	0.17	1.3	
11[f]	0.83	100	0.16	4.9	

[a] Reactions were carried out in a 50 mL Parr hydrogenation reactor at the required conditions at 50 °C. THF was the solvent, and potassium *tert*-butoxide (7.4 mM, C/B = 1/8) was used as the base. [b] The solubilities of H_2 and D_2 were taken from ref 40. [c] Values obtained from the least-squares fits of the data plotted in Figures 2 and 3. [d] Values calculated from the proposed rate law given by eq 1. [e] Reaction conducted using 8 bar of D_2 gas. [f] Reaction conducted using acetophenone-d_3 (0.16 M) and H_2 gas (25 bar).

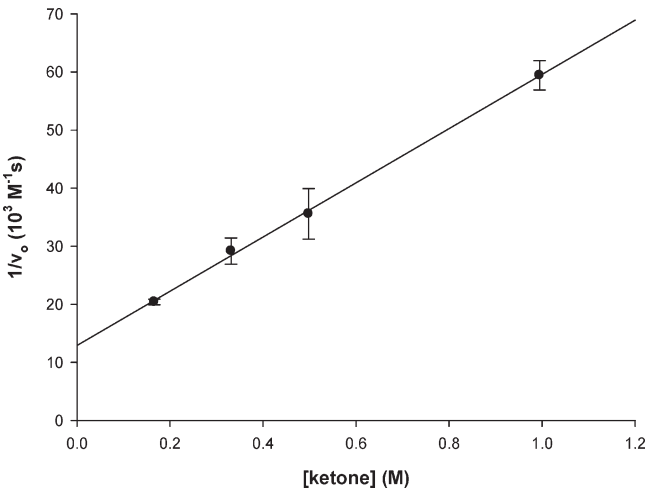

Figure 3. Linear plot showing the relationship between the reciprocal of the initial rate ($1/v_0$ in 10^3 M^{-1} s) and acetophenone concentration (M). The rate (k_H) and equilibrium (K_{eq}) constants were derived from the slope and the y intercept according to eq 2, respectively.

Under pseudo-first-order conditions, it was determined that the rates, within experimental error, are first order in the concentrations of the complex **1** and of hydrogen. A plot of the initial rate (v_0, in M s^{-1}) versus [**1**] (in mM) yielded a straight line with a slope of $(60 \pm 1) \times 10^{-3}$ s^{-1}, while that of v_0 versus $[H_2]$ in THF[40] gave a straight line with a slope of $(48 \pm 1) \times 10^{-5}$ s^{-1}. Each plot passed through the origin. A plot of initial rate (in M s^{-1}) versus [ketone] (in M) yielded a hyperbola which does not pass through the origin (Figure 2) and gave a reaction order of −0.6 on the ketone. The rate law, on the other hand, is zero order in the concentrations of 1-phenylethanol and potassium tert-butoxide within the range of concentrations of interest (vide infra).

Scheme 1. Reaction Scheme Showing the Definitions of the Rate and Equilibrium Constants

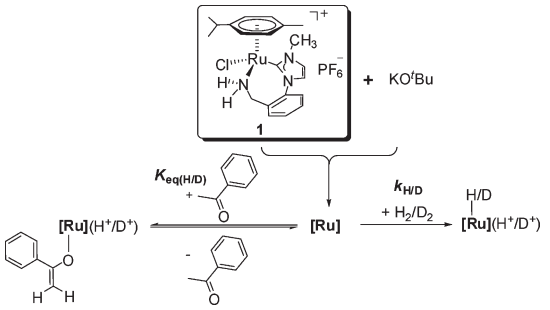

A possible general form of the course of the reaction is proposed as shown in Scheme 1 to explain the kinetic data and the experimental findings. First, an active species is quickly formed by the reaction of complex **1** with a base. This species can then either reversibly react with acetophenone ($K_{eq(H/D)}$) to produce an enolate complex or, in the rate-determining step ($k_{H/D}$), irreversibly react with hydrogen (or deuterium) gas to give a second reactive ruthenium complex responsible for the reduction of the ketone to the product alcohol (Scheme 1). This second complex is likely to be a hydride (or deuteride) formed by the heterolytic splitting of dihydrogen (or dideuterium).

Similar observations were reported in the H_2-hydrogenation of acetophenone using the precatalyst *trans*-RuHCl-(κ^4-(*S,S*)-cyP$_2$(NH)$_2$) when activated by base under 12 bar of H_2 in 2-propanol at 20 °C: a 3-fold increase in the C/S ratio to 1/12 500 led to a decrease in the initial rate by 25%.[26] For the system which might undergo the outer-sphere bifunctional mechanism, it was postulated that a reversible reaction between acetophenone and the ruthenium−amido complex RuH(κ^4-(*S,S*)-cyP$_2$(NH)-(NH$_2$)) forms the ruthenium−ketone adduct, and this equilibrium outcompetes the coordination of dihydrogen to ruthenium. This had the effect of slowing catalysis, since it was proposed that the heterolytic splitting of η^2-H_2 by the amido complex to afford the bifunctional dihydride catalyst *trans*-Ru(H)$_2$(κ^4-(*S,S*)-cyP$_2$(NH$_2$)) was rate-limiting. The binding of the ketone to the amido complex might also lead to the formation of a stable enolate complex: this could occur by the deprotonation of an α-C−H proton from the coordinated acetophenone by the ruthenium−amido complex (Scheme 1).

The rate law (eq 1) can be derived from this general reaction scheme (see the Supporting Information for derivation):

$$\text{rate} = -\frac{\mathrm{d}[\text{ketone}]}{\mathrm{d}t} = \frac{k_H[\text{Ru}]_{tot}[H_2]}{1 + K_{eq}[\text{ketone}]} \qquad (1)$$

in which $[\text{Ru}]_{tot}$ is the total concentration of ruthenium species, after complex **1** is activated with base. This suggests that [**1**] is equal to $[\text{Ru}]_{tot}$ if catalyst decomposition does not occur. By taking the reciprocal of eq 1, the reciprocal of the rate and the ketone concentration is related by eq 2.

$$\frac{1}{\text{rate}} = \frac{1}{k_H[\text{Ru}]_{tot}[H_2]} + \frac{K_{eq}[\text{ketone}]}{k_H[\text{Ru}]_{tot}[H_2]} \qquad (2)$$

This will allow the calculation of k_H and K_{eq} values, respectively, using the slope and the *y* intercept of such a linear plot. Indeed, a plot of the reciprocal of initial rate (in M^{-1} s) versus [acetophenone] (in M) using the kinetic data is linear with a *y* intercept of $(12.9 \pm 0.7) \times 10^3$ M^{-1} s^{-1} and a slope of $(46.6 \pm 1.2) \times 10^3$ M^{-2} s^{-1} (Figure 3). Thus the rate and equilibrium constants obtained using the rate law given in eq 1 for the range of acetophenone, complex **1**, hydrogen, 1-phenylethanol and base concentrations studied are

$$k_H = 0.94 \pm 0.05 \text{ M}^{-1} \text{ s}^{-1}$$

$$K_{eq} = 3.6 \pm 0.2 \text{ at } 323 \text{ K}$$

The K_{eq} value was also used to calculate the rate constant k_H from the plots of initial rate versus [**1**] or [H_2], and the values obtained are within experimental error compared to the value obtained from the plot of reciprocal of initial rate versus [acetophenone]. The observed and calculated initial rates given in Table 3 also are in good agreement.

Effect of the Base on Catalysis. The relationship between the concentration of potassium *tert*-butoxide (KO^{t}Bu) and rates were examined by means of kinetic studies. A plot of initial rate (in M s^{-1}) versus [KO^{t}Bu] (in M) yielded a straight line with a slope of $-(9.5 \pm 1.3) \times 10^{-4}$ s^{-1} which does not pass through the origin (see the Supporting Information, Figure S2). The reaction order was −0.2, as determined by the kinetic data. The concentration of the alkoxide base, therefore, does not greatly influence the rate of catalysis. In addition, potassium *tert*-butoxide in high concentrations is known to form stable aggregates in solvents with low dielectric constants, such as THF. For instance, the reaction of Pt(papH)Cl (papH = κ^3-*C,N,N*-2-phenyl-6-(2-aminoisopropyl)pyridine) with 5 equiv of KO^{t}Bu in benzene afforded the amido complex [Pt(pap)]$_2$(KO^{t}Bu)$_8$(KCl).[41] The chloride anion was encapsulated by seven potassium ions, and the potassium ions were bridged by oxygens of the *tert*-butoxide anions. The decrease in rate in catalysis with an increasing concentration of the base (up to 18 mM) can plausibly be attributed to complex ion-pairing and aggregation effects between cationic potassium and ruthenium species with the anionic *tert*-butoxide, the enolate of acetophenone, and the alkoxide of 1-phenylethanol. Potassium ions are known to form solvates with THF molecules, but these are weak in comparison to strong anion−cation ion-pairing interactions. On the other hand, a decrease in rate was also observed when a low concentration of base (1.2 mM) was used in catalysis (C/B/S = 1/1.4/200).

It has been shown that for certain transfer[42] and H_2-hydrogenation[43] systems, particular alkali-metal cations

(40) This was modeled using the data obtained for 1,2-dimethoxyethane at 323 K. The Henry's Law constant for the solubility of H_2 in THF at 50 °C was therefore modeled to be 3.98×10^{-2} M/bar; see: (a) *Solubility Data Series, Hydrogen and Deuterium, 5/6*; Young, C. L., Ed.; Pergamon Press: New York, 1981. Deuterium gas is 1.046 times more soluble than hydrogen gas in water at 50 °C; see: (b) Muccitelli, J.; Wen, W. Y. *J. Solution Chem.* **1978**, *7*, 257–267.

(41) Song, D.; Morris, R. H. *Organometallics* **2004**, *23*, 4406–4413.

(42) (a) Vastila, P.; Zaitsev, A. B.; Wettergren, J.; Privalov, T.; Adolfsson, H. *Chem. Eur. J.* **2006**, *12*, 3218–3225. (b) Wettergren, J.; Buitrago, E.; Ryberg, P.; Adolfsson, H. *Chem. Eur. J.* **2009**, *15*, 5709–5718.

(43) Hartmann, R.; Chen, P. *Angew. Chem., Int. Ed.* **2001**, *40*, 3581–3585.

can accelerate the catalysis by acting as a Lewis acid. This possibility was examined by our system. The addition of [2.2.2]cryptand in equimolar amount to potassium ions (C/B/S = 1/1.4/200) led to comparable reaction rates with respect to the standard condition for catalysis (C/B/S = 1/8/200). An equimolar amount of 18-crown-6 that was added with respect to base (C/B/S = 1/8/200, [KO^{t}Bu] = 7.4 mM) had no effect on the reaction rate. The use of a base with sodium ions (NaO^{t}Bu, Table 1, entry 3) gave low activity in catalysis. This, however, was attributed to the limited solubility of the base in THF solution. Therefore, the cations of the alkoxide base do not significantly affect the rate of catalysis.[26]

Effect of Alcohols on Catalysis. A plot of initial rate (in M s^{-1}) versus [1-phenylethanol] (in M) added in excess obtained in kinetic studies yielded a straight line with a slope of $(1.1 \pm 0.5) \times 10^{-4}$ s^{-1} which does not pass through the origin (see the Supporting Information, Figure S3). The reaction order was −0.1, as determined by the kinetic data. The product alcohol and 2-propanol, therefore, have minimal effect on catalysis and do not contribute to the rate law. Of note, the rate of conversion was somewhat higher using 2-propanol (Table 1), due to the combined activities of both H_2 and transfer hydrogenation.[38]

Isotope Effects and Deuterium Labeling Studies. The measurement of kinetic isotope effects (KIE)[44] is a powerful technique to gain important mechanistic insight in catalysis. The use of both hydrogen and deuterium gas in the measurement of the kinetic isotope effect for hydrogenation catalysts is common,[17,45] but it is less well known for homogeneous bifunctional catalysts for the H_2-hydrogenation of polar bonds.[16,18] Noyori and co-workers have reported a KIE value (k_H/k_D) of 2 for the hydrogenation of acetophenone catalyzed by *trans*-RuH(η^1-BH$_4$)((*S*)-tolbinap)((*S,S*)-dpen) in the presence of base in H_2/2-propanol versus D_2/2-propanol-d_8.[16] We have recently reported a KIE value of 2.0 ± 0.1 for the hydrogenation of acetophenone catalyzed by *trans*-Ru(H)$_2$((*R*)-binap)(tmen). This was interpreted as an early transition state involving the heterolytic splitting of dihydrogen (dideuterium) by the ruthenium catalyst where there is little weakening of the H−H/D−D bond.[18]

The rates of the reaction using D_2 gas were examined within a given range of acetophenone concentrations (0.083−0.16 M) at low D_2 gas pressure (8 bar) and 50 °C in basic THF to obtain meaningful kinetic data. The k_D and $K_{eq(D)}$ values were calculated from the slope and *y* intercept of a plot of the reciprocal of the initial rate (in M^{-1} s) and [acetophenone] (in M) as in eq 2. This gave a linear plot with a *y* intercept of $(51 \pm 5) \times 10^3$ M^{-1} s^{-1} and a slope of $(15 \pm 4) \times 10^4$ M^{-2} s^{-1}. The catalysis conditions along with the results of the kinetic data and calculated values of k_D and $K_{eq(D)}$ are given in Figure 4, in Tables 3 and 4, and in the Supporting Information (Tables S4 and S5 and Figure S4). The experimentally determined kinetic isotope effect value (k_H/k_D), within experimental error, is 1.33 ± 0.15 for using H_2 versus D_2 gas.

Since the presence of α-C−H groups adjacent to the carbonyl group of a ketone was shown to inhibit catalysis by allowing enolate formation, it was important to determine the effect of deuteration of these positions in acetophenone. Kinetic studies were therefore performed using acetophenone-d_3 (0.16−0.49 M) at 25 bar of H_2 and 50 °C in basic THF. The k_D and $K_{eq(D)}$ values were computed in a fashion similar to that described above by first plotting the reciprocal of initial rate (in M^{-1} s) versus [acetophenone-d_3] (in M, Figure 4) to yield a *y* intercept of $(17 \pm 1) \times 10^3$ M^{-1} s^{-1} and a slope of $(22 \pm 3) \times 10^3$ M^{-2} s^{-1}. The catalysis conditions, results of the kinetic data, and calculated values of k_D and $K_{eq(D)}$ are given in Tables 3 and 4 and in the Supporting Information (Tables S4 and S6 and Figure S5).

The deuterated products were examined by NMR spectroscopy. For catalysis using 8 bar of D_2 gas (C/B/S = 1/8/200) at 50 °C, deuterium incorporation into the methyl groups of the unreacted acetophenone and of the product 1-phenylethanol was observed at 50% conversion by use of ^{1}H (in $CDCl_3$) and ^{2}D NMR analysis, with C_6D_6 serving as an external reference. Deuteration of the phenyl ring as a result of C−H activation of the ketone substrate was not observed. Deuteration by D_2 gas at the alcoholic oxygen and the carbonyl carbon was observed (>81% enrichment). Likewise, for catalysis using acetophenone-d_3 and 25 bar of H_2 gas (C/B/S = 1/8/200) at 50 °C, hydrogen scrambling with deuterium in the methyl group was observed in both acetophenone and 1-phenylethanol at 91% conversion.

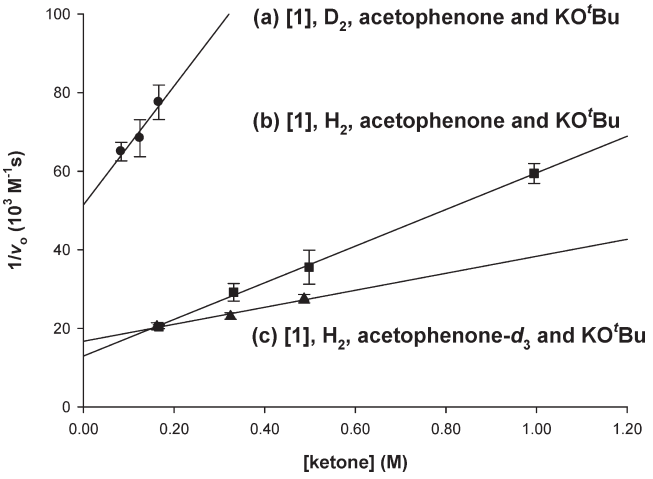

Figure 4. Linear plots showing the relationship between the reciprocal of the initial rate ($1/v_0$ in 10^3 M^{-1} s) and acetophenone concentration (M), using (a) D_2 gas (8 bar) and acetophenone, (b) H_2 gas (25 bar) and acetophenone, and (c) H_2 gas (25 bar) and acetophenone-d_3 (0.16−0.49 M), in the production of 1-phenylethanol from acetophenone catalyzed by complex **1** in basic THF. Details of the reaction conditions are given in Table 3 and in the Supporting Information (Tables S4−S6).

Table 4. Isotope Effect for the Hydrogenation of Acetophenone Catalyzed by Complex 1

deuterium source[a]	k_D (M^{-1} s^{-1})[b]	$K_{eq(D)}$[b]	KIE (k_H/k_D)
D_2 (8 bar, 33 mM)	0.70 ± 0.07	2.9 ± 0.8	1.33 ± 0.15
acetophenone-d_3 (0.16 − 0.49 M)	0.72 ± 0.05	1.3 ± 0.2	1.29 ± 0.11

[a] Reactions were carried out in a 50 mL Parr hydrogenation reactor at the required conditions at 50 °C. THF was the solvent, and potassium *tert*-butoxide (7.4 mM) was used as base. [b] Values obtained from the slopes and intercepts of the linear plots given in Figure 4 and eq 2.

(44) Westheimer, F. H. *Chem. Rev.* **1961**, *61*, 265–273.
(45) (a) Chock, P. B.; Halpern, J. *J. Am. Chem. Soc.* **1966**, *88*, 3511–3514. (b) Brown, J. M.; Parker, D. *Organometallics* **1982**, *1*, 950–956. (c) Kitamura, M.; Tsukamoto, M.; Bessho, Y.; Yoshimura, M.; Kobs, U.; Widhalm, M.; Noyori, R. *J. Am. Chem. Soc.* **2002**, *124*, 6649–6667. (d) Imamoto, T.; Itoh, T.; Yoshida, K.; Gridnev, I. D. *Chem. Asian J.* **2008**, *3*, 1636–1641.

Scheme 2. Possible Outer-Sphere Mechanism That Involves Bifunctional Catalysis in the Hydrogenation of Acetophenone

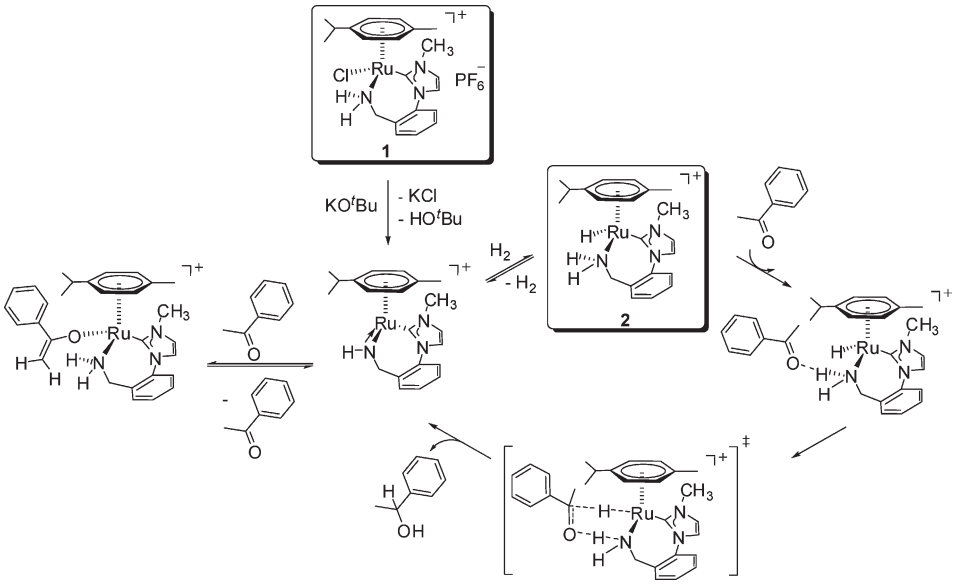

Scheme 3. Synthesis of Complex 2 from Reaction of Complex 1 and Basic 2-Propanol

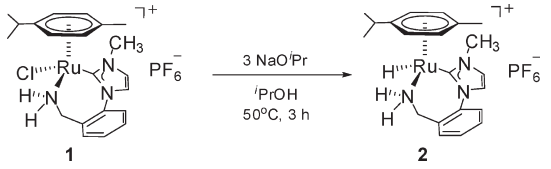

Deuteration at the alcoholic oxygen and the carbonyl carbon was not important in this case (< 3% enrichment). Deuterium scrambling into the methyl group of the acetophenone and 1-phenylethanol may occur via protonation/deuteration of an enolate complex, since a stoichiometric reaction of acetophenone-d_3 and 1-phenylethanol in basic THF under an argon atmosphere at 50 °C also leads to deuterium/proton scrambling in the methyl group of the ketone but not in the alcohol (see the Supporting Information, Figure S6). The former could also occur by H^+/D^+ exchange with the amine ligand or with the alcoholic proton of coordinated 1-phenylethanol or *tert*-butanol. The formation of stable ruthenium(II) complexes containing strong deuterium−heteroatom bonds in the ligands and a strong ruthenium−deuteride bond is thermodynamically favored. This makes the transfer of D^+/D^- to the ketone from the metal difficult.

The use of D_2 and acetophenone-d_3 as deuterium sources helps to confirm the rate law equation and the kinetic model shown in Scheme 1. If the heterolytic splitting of dihydrogen is the rate-determining step in the catalytic cycle, the use of acetophenone-d_3 as a substrate should have a small kinetic isotope effect on k_H but a large isotope effect on the equilibrium between the active species and the enolate complex. This is exactly what is observed. On the other hand, the use of D_2 gas gave a kinetic isotope effect but had little influence on the equilibrium between the active species and the enolate complex. The equilibrium constant values for enolate formation decrease as the number of deuterium atoms available in the system increases on going from the use of a protic source (H_2, acetophenone) to a partially deuterated ketone (H_2, acetophenone-d_3) (Scheme 1 and Table 4). We conclude that the small kinetic isotope effect that is observed upon the use of D_2 gas in the reduction of acetophenone is indicative of an early transition state in the heterolytic splitting of H_2[18] combined with an expected inverse equilibrium isotope effect for the H_2/D_2 binding to the active ruthenium species.[46]

The Disfavored Outer-Sphere Mechanism. Two mechanistic proposals should be considered in light of the experimental findings described above. While the outer-sphere mechanism[9] is expected, there is stronger evidence for an inner-sphere mechanism as described below. In an outer-sphere mechanism which would involve the bifunctional nature of a primary amine group (NH_2) and the metal−hydride bond (Ru−H), the activation of complex **1** with base should give a metal−amido complex containing a trigonal-planar nitrogen donor atom (Scheme 2). Coordination of dihydrogen to such a complex and subsequent heterolytic splitting of the molecule should give the bifunctional metal−hydride and protic amine grouping. The hydride and the proton equivalent would then transfer to the ketone in the outer coordination sphere, giving the product alcohol, without coordination to the metal center. In this mechanism the observed inhibition by enolizable ketones would be explained by the reaction of the ketone with the metal−amido complex.[26] Deprotonation of the methyl group should afford the enolate complex with the primary amine group restored.

In order to identify reaction intermediates in the outer-sphere mechanism, reactions of excess or stoichiometric amounts of base (KO^tBu, KH, $NaBH_4$, or K-Selectride) with complex **1** in THF were tried, but these gave multiple unidentifiable products. Attempts to isolate such products failed and instead led to instant decomposition. Attempts to prepare the ruthenium−hydride complex **2** (Scheme 2) by using dihydrogen (up to 5 bar) in excess KO^tBu in stirring THF at 25 or 50 °C also failed. However, complex **2** could be prepared by warming complex **1** and 3 equiv of sodium

(46) Parkin, G. *Acc. Chem. Res.* **2009**, *42*, 315–325 and references therein.

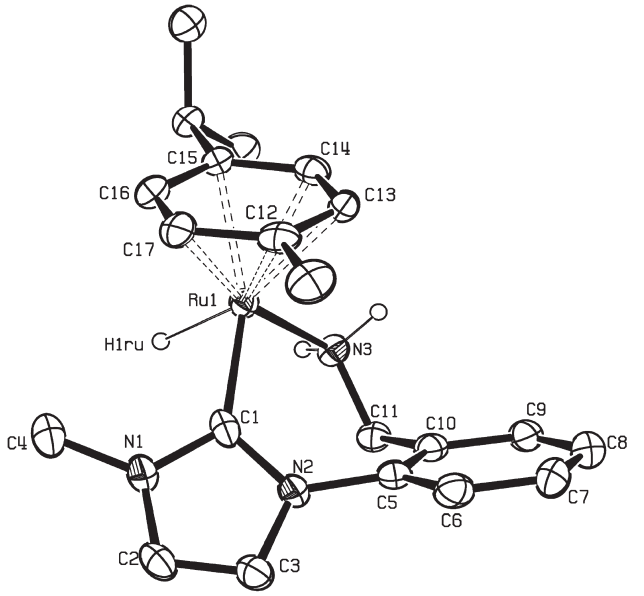

Figure 5. ORTEP diagram of **2** ([Ru(*p*-cymene)(*m*-CH_2NH_2)-H]PF_6) depicted with thermal ellipsoids at the 30% probability level. The counteranion, solvent molecule, and most of the hydrogens have been omitted for clarity. Selected bond distances (Å) and bond angles (deg): Ru(1)−C(1), 2.029(7); Ru-(1)−N(3), 2.145(5); Ru(1)−H(1ru), 1.79(7); Ru(1)−C(12), 2.274(6); Ru(1)−C(15), 2.232(6); C(1)−Ru(1)−N(3), 91.9(2); C(1)−Ru(1)−H(1ru), 81(2); H(1ru)−Ru(1)−N(3), 84(2).

2-propoxide in 2-propanol solution at 50 °C for 3 h, giving a brown solid upon isolation in 57% yield (Scheme 3). The use of KO^{t}Bu or a reaction that was conducted in refluxing 2-propanol gave impure products. Complex **2** is oxygen sensitive both in solution and in the solid state. A solution of **2** in dichloromethane readily converts to the cation of complex **1** at room temperature in hours and slowly reacts with solvents such as acetonitrile after prolonged standing for days.

Complex **2** was unambiguously characterized by an X-ray diffraction study (Figure 5, Table 5). The compound adopts a piano-stool geometry about the metal center. The Ru−$C_{carbene}$ bond (2.029(7) Å) was shorter than that of complex **1** (2.092(5) Å).[38] The large bite angle between the carbene and primary amine donor containing the metal center (C(1)−Ru(1)−N(3) = 91.9(2)°) is typical of L−Ru−L angles for ruthenium arene complexes ([Ru(η^6-arene)HL_2]$^+$) containing a hydride ligand.[7,22,47] Note that the contact distance of 2.45 Å between the ruthenium hydride and the primary amine protons (Ru−H···H−N−) is comparable to that for the complex RuH(η^6-*p*-cymene)((*S,S*)-Tsdpen) (contact distance 2.29 Å) reported by Noyori and coworkers.[7] In solution, the Ru−$C_{carbene}$ resonance was observed at 185.3 ppm in the ^{13}C NMR spectrum. The Ru−H resonance was observed at −7.82 ppm in the ^{1}H NMR spectrum in CD_3CN. This lies in the region for analogous ruthenium−hydride complexes of the type [Ru(η^6-arene)HL_2]$^+$.[7,22,47]

The catalytic activity of the hydride complex **2** was then tested under H_2-hydrogenation (25 bar, 50 °C in THF or 2-propanol) and transfer hydrogenation (75 °C in 2-propanol) conditions. No catalytic activity was observed in the H_2 hydrogenation of acetophenone in the absence of base when a C/S ratio of 1/200 was used. A conversion of 3% to 1-phenylethanol and a maximum conversion of 9% were achieved in 2 and 19 h, respectively, under transfer hydrogenation conditions in the absence of base when the same C/S ratio was used. However, addition of base (KO^{t}Bu) to such a reaction mixture activates the complex to catalyze the hydrogenation of acetophenone. Full conversion to 1-phenylethanol is achieved in 45 min with a C/B/S ratio of 1/8/200 under identical H_2-hydrogenation conditions as above and to 88% conversion in 2 h under identical transfer hydrogenation conditions. Plots of the concentration of product alcohol versus time for both H_2-hydrogenation and transfer hydrogenation were sigmoidal with a short induction period of 6 and 30 min, respectively (Figure 6). The induction period can be explained by the conversion of **2** by reaction with the base into a catalytically active species. The addition of 1-phenylethanol to the starting mixture led to a slower reaction rate and a slightly longer induction period. Therefore, the alcohol does not act as a proton shuttle in the heterolytic splitting of H_2 in the transition state, in contrast to other bifunctional systems that were studied.[2,20,28,39]

Interestingly, the cationic complex **2** containing a ruthenium hydride and primary amine grouping does not transfer its hydride and proton equivalent to a ketone. This was confirmed by the lack of reaction between complex **2** and a stoichiometric amount of acetophenone in THF-d_8 at 25 or 50 °C. It was expected that the metal hydride and a protic amine grouping would be suitable to effect bifunctional catalysis of polar bonds.[2,6,8,9] The use of an N-heterocyclic carbene as the ligand in this cationic complex clearly shows

Table 5. Selected Crystal Data, Data Collection, and Refinement Parameters for 2 and 6[a]

	6	2
empirical formula	$C_{21}H_{27}ClF_6N_3OsP$	$C_{21}H_{28}F_6N_3RuP\cdot C_4H_8O$
fw	692.08	640.61
lattice type	monoclinic	orthorhombic
space group	$P2_1/n$	*Pbca*
T, K	150	150
a, Å	12.7810 (15)	16.8737(3)
b, Å	16.890 (2)	14.6964(6)
c, Å	13.5646 (16)	22.3909(7)
α, deg	90	90
β, deg	113.406(9)	90
γ, deg	90	90
V, Å^3	2687.3(6)	5552.6(3)
Z	4	8
ρ_{calcd}, Mg m^{-3}	1.711	1.533
μ(Mo Kα), mm^{-1}	4.959	0.686
F(000)	1344	2624
cryst size, mm^3	0.20 × 0.08 × 0.02	0.22 × 0.12 × 0.08
θ range collected, deg	2.8−25.0	2.59−25.00
no. of collected/unique rflns	9182/4338	24 408/4879
abs cor	semiempirical from equivalents	
max, min transmission coeff	0.9073, 0.4371	0.960, 0.828
no. of params refined	286	342
goodness of fit	0.933	1.038
R1 ($I > 2\sigma(I)$)	0.0598	0.0568
wR2 (all data)	0.1520	0.1800
peak and hole, e Å^{-3}	1.536 and −1.777	1.556 and −0.630

[a] Definition of *R* indices: R1 = $\sum(F_o - F_c)/\sum(F_o)$; wR2 = $[\sum[w(F_o^2 - F_c^2)^2]/\sum[w(F_o^2)^2]]^{1/2}$.

(47) Chaplin, A. B.; Dyson, P. J. *Organometallics* **2007**, *26*, 4357–4360.

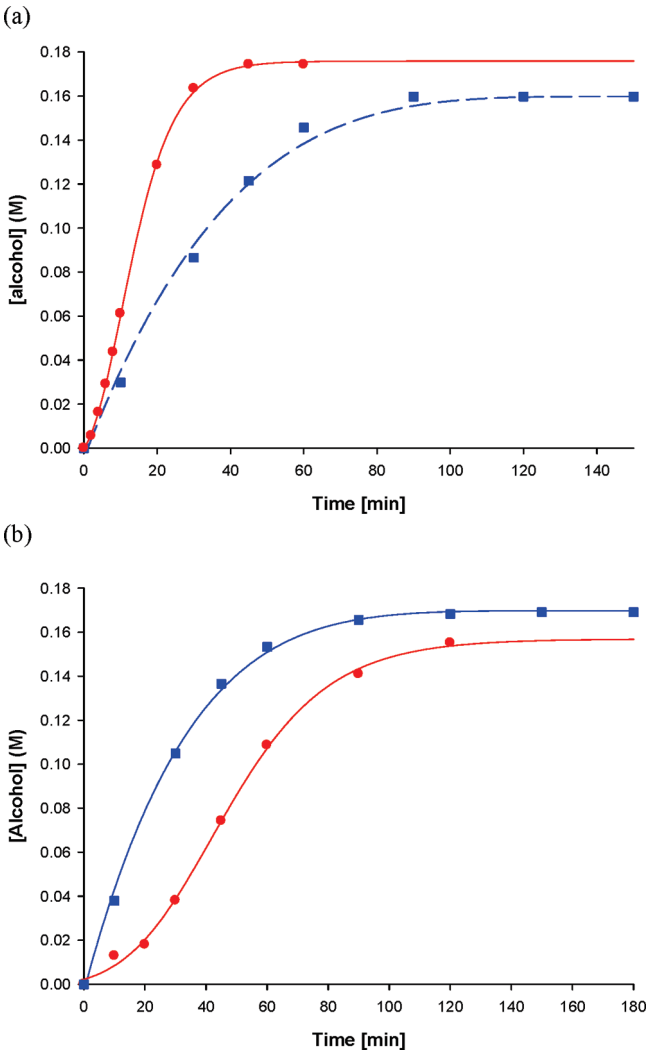

Figure 6. Reaction profiles showing the hydrogenation of acetophenone catalyzed by complex **1** (blue squares) and complex **2** (red circles) in (a) basic THF at 25 bar of H_2 pressure and 50 °C and (b) 2-propanol at 75 °C. The C/B/S ratio was 1/8/200. The transfer hydrogenation of acetophenone catalyzed by complex **1** in basic 2-propanol was reported in ref 38.

that there is no activity in this case. Stradiotto and coworkers have recently reported a highly active zwitterionic ruthenium catalyst containing a phosphine−amine ligand that catalyzes the transfer hydrogenation of ketones in refluxing 2-propanol. On the other hand, the hydride complex of the ruthenium catalyst showed no activity toward ketone reduction, regardless of whether an excess amount of base was added. Such a hydride complex, however, has no protic N−H functionality on its ligand.[22] The cationic charge seems to reduce the nucleophilicity of the hydride ligand so that there is diminished catalytic activity.

If the outer sphere mechanism operates in the H_2-hydrogenation of ketone catalyzed by complex **1** in basic solvents, the hydrogenation of an α,β-unsaturated ketone would most likely afford the reduction of the carbonyl group,[9] although

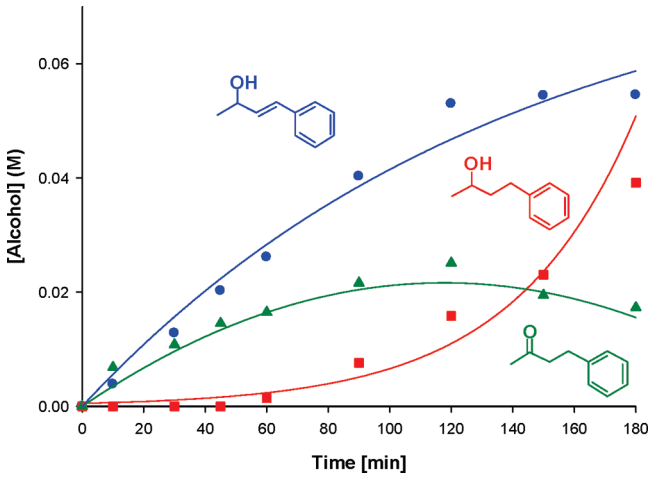

Figure 7. Reaction profile showing the hydrogenation of *trans*-4-phenyl-but-3-en-2-one catalyzed by complex **1** in basic THF at 25 bar of H_2 pressure and 50 °C: (blue circles) *trans*-4-phenylbut-3-en-2-ol; (red squares) 4-phenylbutan-2-ol; (green triangles) 4-phenylbutan-2-one. The C/B/S ratio was 1/8/200.

Scheme 4. Hydrogenation of *trans*-4-Phenyl-but-3-en-2-one Catalyzed by Complex 1

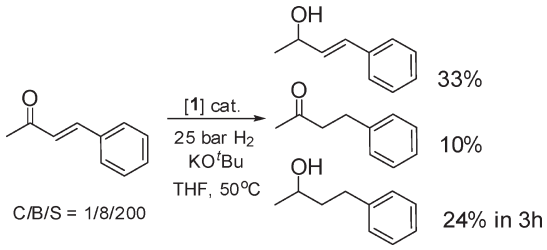

hydrogenation of the conjugated olefin could also occur by a 1,4-addition reaction.[48] A ligand in the active ruthenium species might also rearrange or dissociate to allow the coordination of the olefin and its reduction to occur. This was tested using *trans*-4-phenyl-but-3-en-2-one as the substrate (Scheme 4). Under similar catalytic conditions (C/B/S = 1/8/200, 25 bar of H_2 at 50 °C), complex **1** catalyzed the reduction of the polar bond and the olefin, giving the products *trans*-4-phenyl-but-3-en-2-ol (33% conversion), 4-phenylbutan-2-one (10% conversion), and the fully hydrogenated product 4-phenylbutan-2-ol (24% conversion) in 3 h (Scheme 4 and Figure 7).

The Favored Inner-Sphere Mechanism. Given the experimental data that are not supportive of the outer-sphere mechanism, an inner-sphere mechanism is proposed.[9,49] The ketone must coordinate to the metal center to allow the hydride migration from the metal to the carbonyl group. To effect coordination of the ketone, the primary amine group can decoordinate from the metal center, or the arene ligand on the ruthenium center can slip to η^4 coordination (Figure 8). Of note, a seven-membered ring is formed with the chelating primary amine−NHC ligand, including the nitrogen and carbene donor and the metal center. Facile coordination and recoordination of the tethered group can occur under catalytic conditions. This has been proposed for

(48) (a) Ito, M.; Kitahara, S.; Ikariya, T. *J. Am. Chem. Soc.* **2005**, *127*, 6172–6173. Michael addition reactions catalyzed by bifunctional catalysts can also occur via 1,4-addition without prior coordination of the conjugated olefin to the metal center; see: (b) Ikariya, T.; Gridnev, I. D. *Chem. Rec.* **2009**, *9*, 106–123.

(49) Daley, C. J. A.; Bergens, S. H. *J. Am. Chem. Soc.* **2002**, *124*, 3680–3691.

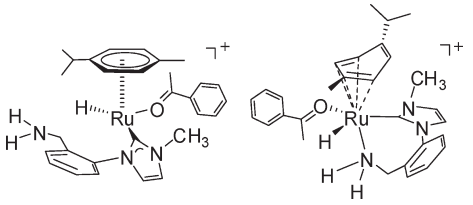

Figure 8. Possible reaction intermediates for the inner-sphere mechanism involving hydride migration to the coordinated ketone substrate: (left) decoordination of the chelating amine group from the NHC ligand; (right) ring slippage of the arene ring.

the transfer hydrogenation of ketones using a complex of type Ru(η^6-arene)(κ^2-N-N)Cl (N-N = 2-hydroxylphenylbis-(pyrazol-1-yl)methane and other derivatives) under base-free conditions. The authors proposed that a nitrogen donor of a pyrazolyl group decoordinates from the metal center during catalysis and acts as a base in the deprotonation of the coordinated alcohol.[50] Elsevier and co-workers recently reported the use of N-heterocyclic carbene complexes with a tethered tertiary-amine group of palladium(0), [Pd(NHC-amine)(alkene)], in the transfer hydrogenation of alkynes to (*Z*)-alkenes under base-free conditions. Experimental findings suggest the tethered amine group dissociates from the metal center and acts as a base in catalysis.[51] Chu and co-workers reported the use of a half-sandwich complex of ruthenium containing a tethered tertiary amine group on the cyclopentadienyl ligand, which acts as a base to assist the heterolytic cleavage of dihydrogen.[52] Nolan and co-workers have recently reported the mechanism of racemization of chiral alcohols catalyzed by ruthenium(II) systems containing N-heterocyclic carbene ligands. This was suggested to undergo an inner-sphere mechanism which involved the dissociation of a coordinated carbonyl ligand. An Ru−O(alkoxide) bond was formed in the presence of alkoxide, and this is responsible for the formation of a ruthenium hydride intermediate in the racemization of chiral alcohol. This is further supported by NMR studies and DFT computations.[53] The feasibility of the amino group dissociation has been explored using computational methods (vide infra). Of note, it is less likely for the primary amine group to act as a base in catalysis, as complex **1** must be activated by an alkoxide base to become active.

In order to probe the importance of the primary amine group tethered to the N-heterocyclic carbene ligand in complex **1**, we attempted to make and test the *N,N*-dimethylamine analogue. Methylation of the primary amine group of complex **1** was not successful. We did succeed in preparing a closely related compound by reaction of the imidazolium salt **3**[54] with silver(I) oxide and [Ru(*p*-cymene)Cl_2]$_2$ in one pot (Scheme 5). Note that the carbene ligand derived from **3**, if it chelates to the metal, will form a seven-membered ring as observed in complex **1**. The in situ generation of the silver(I) carbene complex derived from **3** and subsequent transmetalation of the NHC ligand to ruthenium(II),[55] followed by counteranion metathesis, gave a compound formulated on the basis of elemental analysis as [Ru(*p*-cymene)Cl-($CH_3NC_3H_2N(CH_2)_3N(CH_3)_2$)]$PF_6$·1.5 DMSO (**4**). The use of DMSO as cosolvent for the reaction is unavoidable, as ligand **3** has limited solubility in most organic solvents except alcohols. Attempts to isolate the intermediate silver(I) carbene complex containing the corresponding imidazolylidene ligand failed, as this quickly decomposed.

The NMR spectra of **4** in CD_2Cl_2 at 253 K indicate that compound **4** is a mixture of two complexes, one with a chelating NHC ligand and another with a nonchelating NHC and coordinated DMSO ligand. Infrared spectroscopy usually provides a means of distinguishing between O- and S-bound forms of the dimethyl sulfoxide ligand[56] but did not prove helpful because of the complex spectrum in the fingerprint region (see the Supporting Information, Figure S7). The experimental procedures and the characterization of the compounds are given in the Supporting Information.

Complex **4** is an effective catalyst for the H_2-hydrogenation of acetophenone with an activity comparable to that of complex **1** under similar reaction conditions (C/B/S = 1/10/240, 25 bar of H_2 at 50 °C) in basic THF with KO^{t}Bu as a base. A conversion of 76% to 1-phenylethanol was achieved within 2 h of reaction. Like complex **1**, no induction period was observed (see the Supporting Information, Figure S8). Therefore, the protons of the amino group in complex **1** are not needed for catalysis. This is another example showing that the "NH effect" is not always operational in catalysts for polar bond hydrogenation.[21,22]

Theoretical Considerations. The catalytic cycles involved in both outer- (Scheme 2) and inner-sphere mechanisms (Figure 8 and below) were investigated by using density functional theory (DFT) methods. A MPW1PW91 functional was chosen, as this gave better predictions of energy barriers and transition states.[57] For computational ease, the *p*-cymene ligand was simplified to a benzene ligand. The alkoxide base, 1-phenylethanol, and acetophenone were simplified to 2-propoxide, 2-propanol, and acetone, respectively. The cations of the base and the counteranions of the catalytically active species were omitted throughout the calculations.

The reaction coordinate diagram for the outer-sphere mechanism is given in Figure 9. The ruthenium−amido complex $\mathbf{A_1}$ reacts with dihydrogen to give the η^2-dihydrogen complex **B**. The amido nitrogen of $\mathbf{A_1}$ is highly charged (APT charge −0.37 ESU; Table S8 in the Supporting Information) and has a short Ru−N bond (1.89 Å, Figure 10). The sum of the angles around nitrogen is 358° in the optimized structure. Therefore, the nitrogen is sp^2 hybridized and the Ru−N has a double-bond character. The Ru−N bond is longer in **B** (2.09 Å) and the double-bond character is lost, which allows dihydrogen coordination to the coordinatively unsaturated complex. The energy barrier at 298 K and 1 atm for the dihydrogen addition to $\mathbf{A_1}$ on going from structure **B′**, which has the dihydrogen molecule outside the coordination

(50) Carrion, M. C.; Sepulveda, F.; Jalon, F. A.; Manzano, B. R.; Rodriguez, A. M. *Organometallics* **2009**, *28*, 3822–3833.
(51) (a) Warsink, S.; Hauwert, P.; Siegler, M. A.; Spek, A. L.; Elsevier, C. J. *Appl. Organomet. Chem.* **2009**, *23*, 225–228. (b) Hauwert, P.; Boerleider, R.; Warsink, S.; Weigand, J. J.; Elsevier, C. J. *J. Am. Chem. Soc.* **2010**, *132*, 16900–16910.
(52) Chu, H. S.; Lau, C. P.; Wong, K. Y.; Wong, W. T. *Organometallics* **1998**, *17*, 2768–2777.
(53) Bosson, J.; Poater, A.; Cavallo, L.; Nolan, S. P. *J. Am. Chem. Soc.* **2010**, *132*, 13146–13149.
(54) Jimenez, M. V.; Perez-Torrente, J. J.; Bartolome, M. I.; Gierz, V.; Lahoz, F. J.; Oro, L. A. *Organometallics* **2008**, *27*, 224–234.
(55) Warsink, S.; de Boer, S. Y.; Jongens, L. M.; Fu, C. F.; Liu, S. T.; Chen, J. T.; Lutz, M.; Spek, A. L.; Elsevier, C. J. *Dalton Trans.* **2009**, 7080–7086.
(56) James, B. R.; Morris, R. H. *Can. J. Chem.* **1980**, *58*, 399–408.
(57) Lynch, B. J.; Truhlar, D. G. *J. Phys. Chem. A* **2001**, *105*, 2936–2941.

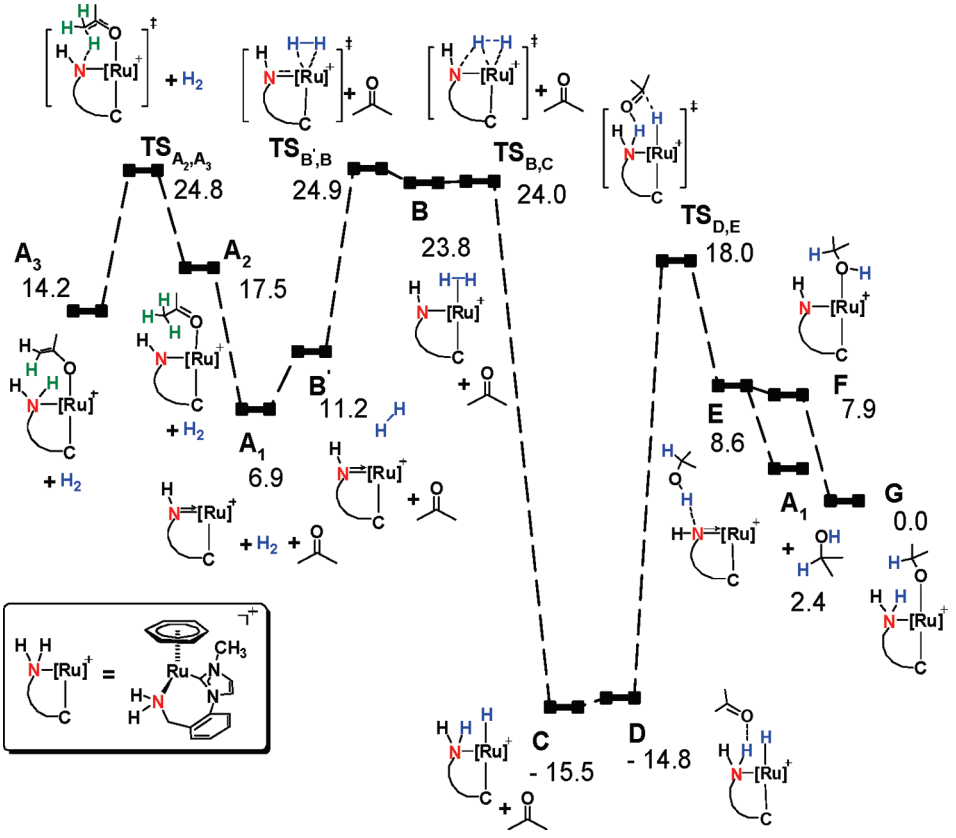

Figure 9. Reaction coordinate diagram for an outer-sphere mechanism for the H_2-hydrogenation of acetone starting from $\mathbf{A_1}$ and moving to the right and the enolate formation starting from $\mathbf{A_1}$ and moving to the left. The free energies are reported relative to **G** in kcal/mol. All computed structures were optimized at 1 atm and 298 K in the gas phase.

Scheme 5. Synthesis of Complex 4 by in Situ Generation of the Silver(I) Carbene Complex and Subsequent Transmetalation of the NHC Ligand to Ruthenium(II)

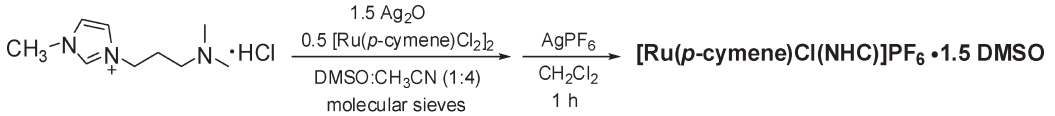

3 **4**

sphere, to the transition state $\mathbf{TS_{B',B}}$ is 18.0 kcal/mol uphill. The entropy change ($\Delta S^{\ddagger}$) for dihydrogen coordination is −25.9 cal/(mol K). The dihydrogen is weakly activated in the transition state and also in structure **B**, as the H−H distances are short (0.76 and 0.83 Å, respectively).[58] Structure **B** leads to the transition state $\mathbf{TS_{B,C}}$, in which the H−H distance increases to 0.88 Å and the negative charge on nitrogen increases from −0.37 to −0.40 ESU. Note that the energy difference between **B** and $\mathbf{TS_{B,C}}$ is only 0.2 kcal/mol.

The heterolytic splitting of H_2 by $\mathbf{A_1}$ leads to **C**, which is −39.5 kcal/mol downhill from $\mathbf{TS_{B,C}}$. The Ru−H distance is 1.58 Å, which is similar within the ESD to the value of the Ru−H distance (1.79(7) Å) in the crystal structure of complex **2**. The single-bond character of Ru−N is retained (2.16 Å), and the charge on nitrogen is further reduced to −0.24 ESU. The charges on ruthenium and hydride are −0.72 and −0.042 ESU, respectively. The smaller charge on the hydride may explain the poor activity of complex **2** toward reaction with acetophenone. The hydrides of the model complex of a ketone hydrogenation catalyst, (*OC*-6-22)-$Ru(H)_2(PH_3)_2(en)$, have charges of −0.20 and −0.15 ESU.[18] From structure **C**, acetone is hydrogen-bonded to the complex, forming **D**, and this goes +33.5 kcal/mol uphill from **C** plus acetone at 298 K and 1 atm, leading to the transition state $\mathbf{TS_{D,E}}$, where the concerted transfer of dihydrogen to the ketone from Ru−H and $Ru-NH_2$ occurs via a six-membered-ring transition state.[9−11] The Ru−H bond is elongated (to 1.84 Å), as is the N−H bond (from 1.02 to 1.30 Å). In addition, the C−H and C−O bonds of the alcohol are formed simultaneously, with bond distances of 1.27 and 1.33 Å, respectively. The charge of ruthenium is reduced (−0.32 ESU) and the hydride is more negatively charged (−0.43 ESU). This leads to the ruthenium−amido−isopropyl alcohol adduct **E**, held by weak electrostatic interactions. The elimination of the alcohol product results in the regeneration of the amido complex $\mathbf{A_1}$, which is −15.6 kcal/mol downhill from $\mathbf{TS_{D,E}}$. The alcohol could also coordinate to the amido complex, forming **F**. Subsequent deprotonation of the alcohol by the amide ligand causes the formation of the ruthenium−alkoxide complex **G**. This has a basic alkoxide ligand (APT charge on O −0.82 ESU) and is more thermodynamically stable than $\mathbf{A_1}$ plus 2-propanol by 2.4 kcal/mol. Of note, the Ru−C(carbene) bond

(58) Morris, R. H. *Coord. Chem. Rev.* **2008**, *252*, 2381–2394.

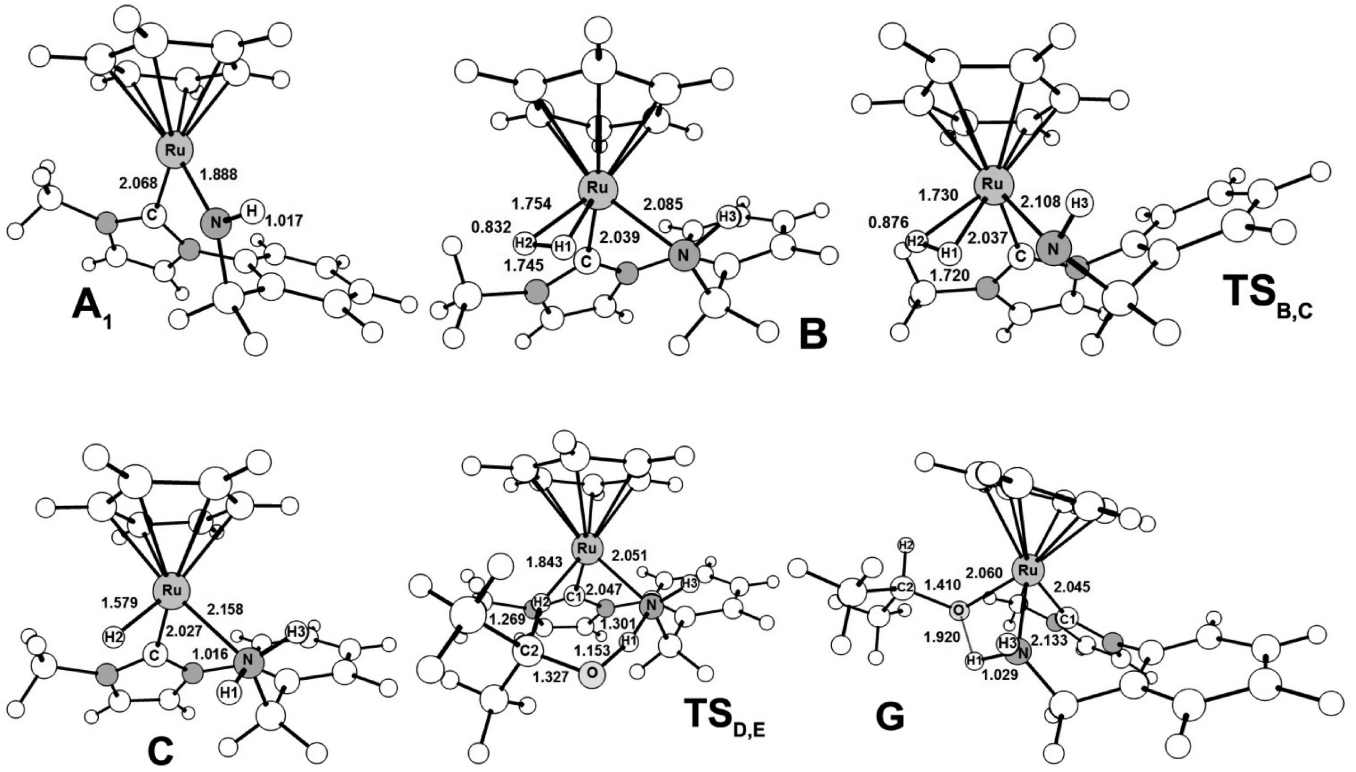

Figure 10. Selected computed structures **A**−**C** and **G** for the outer-sphere mechanism in the H_2-hydrogenation of acetone and the transition state structures for the heterolytic splitting of H_2 (**$TS_{B,C}$**) and for the concerted transfer of a hydride/proton pair to the ketone (**$TS_{D,E}$**). The bond lengths (Å) are given in the structures. The APT charges (ESU) of these structures are given in Table S8 in the Supporting Information.

distances vary from 2.03 to 2.08 Å for all the computed structures, and they are comparable to those of complexes **1** and **2** in the crystal structures (Figure 10).[38]

The enolate complex $\mathbf{A_3}$ is formed from $\mathbf{A_1}$ via coordination of acetone, giving $\mathbf{A_2}$, and this leads to the transition state $\mathbf{TS_{A2,A3}}$, where deprotonation of the methyl group occurs. This is +17.9 kcal/mol uphill from $\mathbf{A_1}$ plus acetone. The product $\mathbf{A_3}$ is thermodynamically less stable than $\mathbf{A_1}$ plus acetone by 7.3 kcal/mol (Figure 9). The computations thus accurately reflect comparable energy barriers for the H_2 addition and enolate formation from the amido complex $\mathbf{A_1}$ (18.0 versus 17.9 kcal/mol at 298 K and 1 atm). The concerted transfer of H^+/H^- to acetone has a much higher barrier of +33.5 kcal/mol in comparison to the aforementioned steps, which contradicts the experimental findings. The calculation also predicts that the ruthenium−hydride complex **C** (or complex **2**) is the resting state of the catalytic cycle. This is more stable than the ruthenium−alkoxide and ruthenium−amido complexes by 15.5 and 22.4 kcal/mol.

An alternative proposal is the inner-sphere mechanism, which involves the decoordination of the amine group from the NHC ligand or ring slippage of the coordinated arene ring.[10] The computed structures of the latter have higher energies (>25 kcal/mol with respect to structure **G**). The ring slipped structures were also higher in energy than those structures computed for the mechanism involving the decoordination of the amine group (see below). Thus, they are not considered as the possible intermediates (the structures and their energies are given in the Supporting Information).

Starting from the alkoxide complex **G**, the decoordination of the amine group is an uphill process by +15.5 kcal/mol at 298 K and 1 atm (Figure 11). This process is entropically favored (ΔS = 16.6 cal/(Mol K)). This afterward provides the coordinatively unsaturated complex **H**, which has a short Ru−O distance compared to **G** (1.90 and 2.06 Å, respectively, Figures 10 and 12). The charges on the oxygens of the alkoxide are comparable in **H** and **G** (−0.82 and −0.77, respectively; Tables S8 and S9 in the Supporting Information). The variation in the Ru−C(carbene) bond distance is similar to that of the outer-sphere mechanism for all of the computed structures (Figure 12). In addition, the Ru−N(amine) distances are more than 5.0 Å for all of the computed structures. For all, the dihedral angle of the phenyl and the imidazolidene rings range from 83.3° for **H** and 95.0° for **K**. For comparison, the dihedral angles for the crystal structures of complexes **1** and **2** are 54.6 and 54.3°.[38]

Coordination of molecular hydrogen in a side-on fashion to **H** then occurs, giving **I**. Both QST3 and QST2 searches were performed, but these failed to locate a transition state for dihydrogen addition to **H**. The dihydrogen is again weakly activated in **I** with a short H−H distance of 0.85 Å.[58] This process works against entropy (ΔS = −16.0 cal/(mol K)). Heterolytic splitting of η^2-H_2 takes place through transition state $\mathbf{TS_{I,J}}$. The H−H distance increases to 0.92 Å, and the charge on oxygen increases from −0.68 to −0.73 ESU. The energy barrier for the heterolytic splitting of H_2 is +33.0 kcal/mol uphill from **G** plus dihydrogen or +17.5 kcal/mol from **H** plus dihydrogen at 298 K and 1 atm. The energy difference between **I** and $\mathbf{TS_{I,J}}$ is 3.7 kcal/mol, indicative of an early transition state. Again, the heterolytic

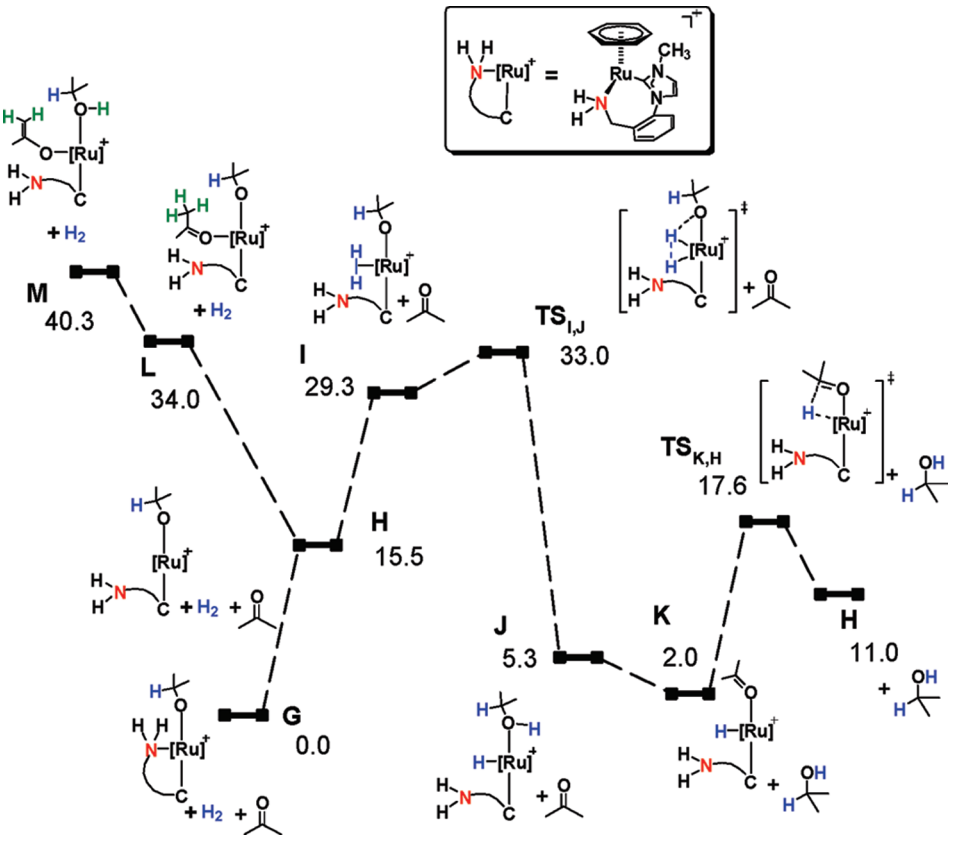

Figure 11. Reaction coordinate diagram for the inner-sphere mechanism in the H_2-hydrogenation of acetone starting from **H** and moving to the right. The amino group is decoordinated and is not involved in hydrogen bonding. Moving to the left from **H** leads to the unstable enolate complex **M**. The free energies are reported relative to **G** in kcal/mol. All computed structures were optimized at 1 atm and 298 K in the gas phase.

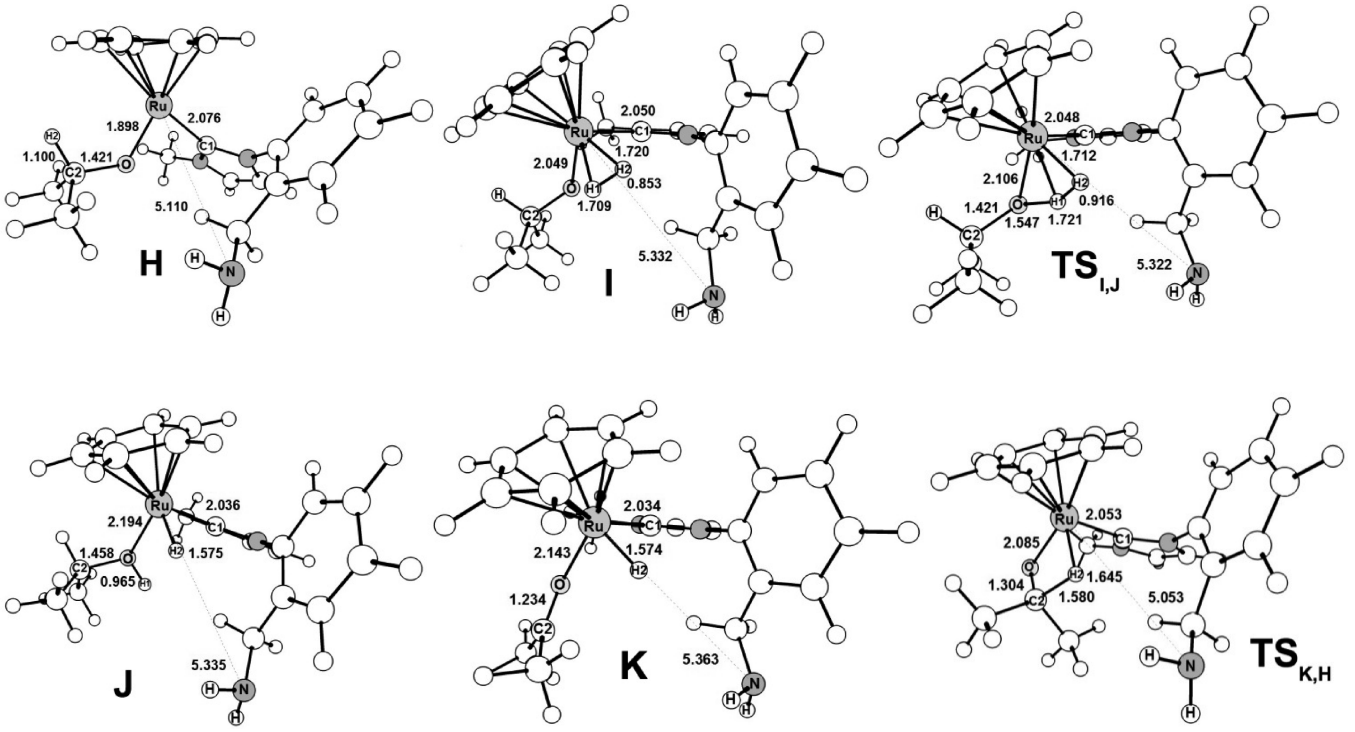

Figure 12. Selected computed structures **H**−**K** for the inner-sphere mechanism involving decoordination of the amine group of the NHC ligand in the H_2-hydrogenation of ketone and the transition state structures for the heterolytic splitting for H_2 (**TS$_{I,J}$**) and for the hydride attack on the coordinated ketone (**TS$_{K,H}$**). The bond lengths (Å) are given in the structures. The APT charges (ESU) of these structures are given in Table S9 in the Supporting Information.

splitting of H_2 is entropically demanding ($\Delta S^{\ddagger} = -19.9$ cal/(mol K)).

The ruthenium−hydride complex containing a coordinated alcohol is then formed from $\mathbf{TS_{I,J}}$, leading to **J**, which is −27.7 kcal/mol downhill. The structure has a short Ru−H bond (1.57 Å). The charges on the ruthenium and the hydride are −0.52 and −0.039 ESU. Decoordination of 2-propanol and recoordination of acetone forms **K**, and a further energy of +15.6 kcal/mol uphill is required, leading to the transition state $\mathbf{TS_{K,H}}$. The hydride ligand on the ruthenium complex attacks the coordinated acetone via a four-membered-ring transition state.[9,53] The Ru−H bond elongates to 1.65 Å and the Ru−O bond shortens (from 2.14 to 2.09 Å), due to an increased charge on oxygen (from −0.57 to −0.60 ESU; Table S9 in the Supporting Information). Likewise, the C−H (1.58 Å) and C−O (1.30 Å) bonds of the alcohol are formed simultaneously. The charge of ruthenium is reduced (−0.70 ESU), and the hydride is more highly charged (−0.10 ESU). This leads to structure **H** and completes the cycle. We are aware of the presence of the geometric isomers of these structures: in particular, in which the amine proton forms a hydrogen bond with the oxygen on the alkoxide or alcohol groups. These have higher energies compared to those described above. A QST3 search in the transition state of the heterolytic splitting of dihydrogen failed to locate any imaginary frequency. The energies and the geometries of such structures are given in the Supporting Information.

The enolate complex **M** is formed from **H** upon coordination of acetone and subsequent deprotonation of the coordinated alkoxide base. No transition state is located between structures **L** and **M**. This is +24.8 kcal/mol uphill starting from **H**. All this reflects different energy barriers for the H_2-splitting and enolate formation from **H** (17.5 versus 24.8 kcal/mol at 298 K and 1 atm). The hydride migration step has a lower energy barrier of 19.6 kcal/mol, which coincides with the experimental findings. Of note, the energy barrier for H_2-splitting starting from the alkoxide **G** plus dihydrogen is even higher (+33.0 kcal/mol), and the computations predict that this is the resting state of the catalytic cycle. This predicts that the heterolytic splitting of dihydrogen is truly the rate-determining step. The formation of an enolate complex, on the other hand, should occur via the amido complex, as the energy barrier is 24.8 kcal/mol uphill starting from **G** and moving successively from $\mathbf{A_1}$ to $\mathbf{A_2}$, to the transition state $\mathbf{TS_{A2,A3}}$, and then to $\mathbf{A_3}$ (see Figure 9). This has a much lower energy barrier than that starting from **H**. Of note, the amido complex could form initially from the alkoxide complex and deprotonation of the amine proton by the internal alkoxide base. Bergens and co-workers proposed a similar mechanism for the complex RuH(OR)(diamine)((*R*)-binap).[15,30]

Possible Mechanism for Transfer Hydrogenation. The computations also gave important information on the transfer hydrogenation of ketones.[38] The transfer hydrogenation might proceed via the outer-sphere mechanism starting from the amido complex $\mathbf{A_1}$, then to **E**, $\mathbf{TS_{D,E}}$, and **D**, and finally to **C**, the ruthenium−hydride complex (Figure 9). The energy barrier starting from $\mathbf{A_1}$ plus 2-propanol is +15.6 kcal/mol uphill at 298 K and 1 atm. The concerted transfer of H^+/H^- proceeds in a manner identical with that described for the H_2-hydrogenation, going from **C** to $\mathbf{A_1}$, with an energy barrier of +33.5 kcal/mol. This high barrier argues against this mechanism, and in fact, the ruthenium−hydride complex **2** has very low activity under transfer hydrogenation conditions in the absence of base.

For the inner-sphere mechanism, decoordination of the amine group of the NHC ligand takes place from the 2-propoxide complex **G** to allow the β-hydride elimination to take place, forming **H**. This proceeds through the transition state $\mathbf{TS_{K,H}}$, leading to the hydride complex **K** (Figure 11). The β-hydride elimination of the alkoxide is uphill by 6.6 kcal/mol from **H**. The hydride ligand from **K** can then attack the carbonyl group of the substrate; this is the same step as described in the inner-sphere H_2 hydrogenation mechanism, with the same energy barrier of +15.6 kcal/mol uphill (Figure 11). Overall, this has lower energy barriers compared with the outer-sphere mechanism and seems more likely to occur during catalysis.

Role of Complex 2 in Catalysis. Complex **2** is not likely to be an intermediate in the H_2-hydrogenation reaction, as attempts to prepare this from complex **1** in basic THF under H_2 failed. In addition, it does not react with acetophenone (see below). This, however, may be the resting state of the catalyst in the transfer hydrogenation, as it can be prepared under similar catalytic conditions. According to the calculations, the amine group of structure **K** can recoordinate, which displaces the coordinated acetone to give structure **C**, which is analogous to complex **2**. This is −33.1 kcal/mol downhill from the transition state $\mathbf{TS_{H,K}}$. The fact that a base is needed to activate complex **2** in both H_2-hydrogenation and transfer hydrogenation reactions is difficult to explain. In fact, a stoichiometric reaction of complex **2** and KO^tBu in THF-d_8 at 50 °C under argon produces a reaction mixture that lacks a hydride signal in the ^1H NMR spectrum. Subsequent addition of a stoichiometric amount of acetophenone to this reaction mixture did not lead to the formation of 1-phenylethanol or 1-phenylethoxide. The species that is formed from the reaction of complex **2** and an alkoxide base may be responsible for the activation of H_2.

Synthesis of an Osmium(II) Complex with an NHC and a Primary Amine Donor. For comparison, the osmium(II) complex **6** was synthesized by transmetalation[38] of the chelating ligand (C−NH_2) from complex **5** to $[Os(p\text{-cymene})Cl_2]_2$[59,60] in refluxing acetonitrile solution (Scheme 6). An air-stable yellow solid was isolated in 93% yield. The X-ray crystal structure of the complex showed a piano-stool geometry about the metal center with an η^6-cymene ligand and the chloro and the chelating C−NH_2 ligands (Figure 13 and Table 5). The Os−$C_{carbene}$ bond (2.07(1) Å) is comparable to those in compounds containing an NHC ligand reported in the literature.[60−62] A diagnostic ^{13}C NMR feature of complex **6** in solution is the Os−$C_{carbene}$ resonance at 159.4 ppm, which lies in the expected range for analogous complexes.[60−62]

The catalytic activity of complex **6** in the hydrogenation of acetophenone was tested using reaction conditions similar to those for the ruthenium(II) complex **1**. The complex, when activated by base (KO^tBu) in THF, gave 23% conversion to 1-phenylethanol using 25 bar of H_2 as the hydrogen source (C/B/S = 1/8/200) in 3 h at 50 °C. It gave 99% conversion in

(59) Cabeza, J. A.; Maitlis, P. M. *Dalton Trans.* **1985**, 573–578.
(60) Castarlenas, R.; Esteruelas, M. A.; Onate, E. *Organometallics* **2005**, *24*, 4343–4346.
(61) (a) Eguillor, B.; Esteruelas, M. A.; Olivan, M.; Puerta, M. *Organometallics* **2008**, *27*, 445–450. (b) Castarlenas, R.; Esteruelas, M. A.; Lalrempuia, R.; Olivan, M.; Onate, E. *Organometallics* **2008**, *27*, 795–798.
(62) Castarlenas, R.; Esteruelas, M. A.; Onate, E. *Organometallics* **2008**, *27*, 3240–3247.

Scheme 6. Synthesis of Osmium(II) Complex 6 by Transmetalation of the C−NH_2 Ligand from 5

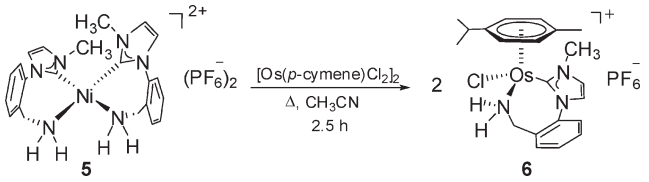

20 h at 50 °C if 2-propanol was used as solvent. On the other hand, the activated complex catalyzed the transfer hydrogenation of acetophenone to 40% conversion to the product alcohol in 18 h at 75 °C (C/B/S = 1/8/200). This has lower activity in the transfer hydrogenation of acetophenone in 2-propanol solution compared to that of complex **1**[38] and analogous systems reported in the literature.[62,63] The poor activity of complex **6** when activated in comparison to **1** might be attributed to the oxophilic nature of the metal center to form stable osmium(II)-alkoxide complexes. Of note, the osmium(II) complex showed no activity when it is not activated by potassium *tert*-butoxide. Similar DFT calculations were also performed with the osmium(II) complex using the inner-sphere mechanism. The osmium(II) dihydrogen complex with a decoordinated amine group similar to **I** is 30.7 kcal/mol uphill from the alkoxide complex analogous to **G** plus dihydrogen (see the Supporting Information). The related complex [Os(*p*-cymene)(NHC)(OH)]OTf (NHC = bis(2,6-diisopropylphenyl)imidazolidene, IPr), was believed to undergo an inner-sphere mechanism for the transfer hydrogenation of aldehydes in 2-propanol solution, whereas the hydroxyl ligand acts as an internal base in the formation of an Os−O(alkoxide) bond.[62]

Conclusion

In summary, the H_2-hydrogenation of ketones catalyzed by complex **1** was studied and the mechanism of action was investigated by both experimental and theoretical means. The ruthenium−hydride complex **2**, which was thought to be the crucial intermediate for bifunctional catalysis, was isolated. This, however, showed no activity under catalytic conditions unless when activated by a base. This hydride complex is believed to be the resting state in the transfer hydrogenation mechanism. The cationic charge on the metal center is likely to decrease the nucleophilicity of the hydride ligand. In fact, this is a rare example of a catalyst with an M−H and N−H grouping that fails to undergo bifunctional catalysis using the "NH effect", which was originally proposed by Noyori and co-workers.[8] Kinetic studies including the studies of isotope effects using D_2 gas and acetophenone-d_3 support the theoretical predictions that an early transition state in the heterolytic splitting of H_2 is the rate-determining step of the catalytic cycle. The outer-sphere mechanism involving bifunctional catalysis of ketone reduction is disfavored according to experimental studies. Computational studies also suggest a high energy barrier for the concerted transfer of H^+/H^- to the ketone compared to dihydrogen addition and subsequent heterolytic splitting.

An alternative to the outer-sphere bifunctional mechanism is therefore proposed on the basis of experimental and theoretical findings. First, complex **1,** when activated, leads to a ruthenium−alkoxide complex. The alkoxide ligand labilizes the cis amine ligand.[64] Decoordination of the amine group of the NHC ligand provides a vacant site for the coordination of dihydrogen (Scheme 7). Ring-opening reactions are common for chelating ligands that form a seven-membered ring with the metal. Catalysis then proceeds with the heterolytic splitting of dihydrogen by the internal alkoxide base, and then hydride attacks the coordinated ketone. In addition, the alkoxide complex can convert to the ruthenium−amido complex which is responsible for the formation of an enolate complex. The current study should assist in the rational design of more robust and active hydrogenation catalysts using N-heterocyclic carbenes as ligands.

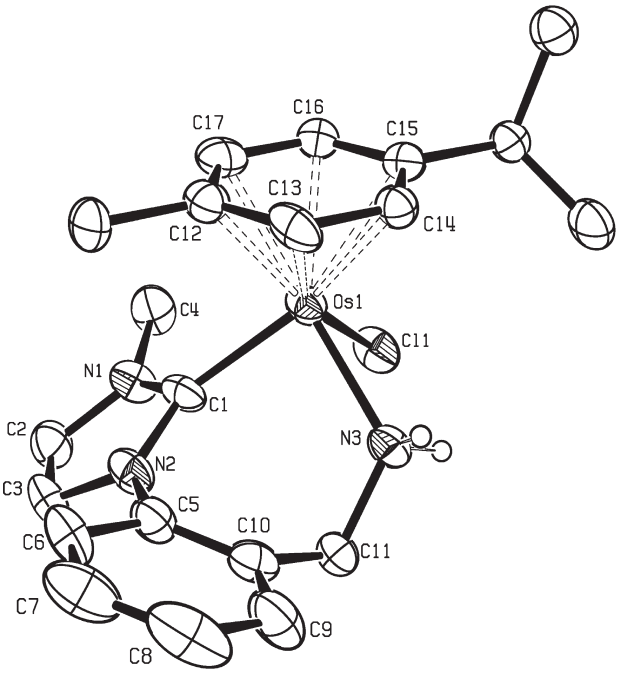

Figure 13. ORTEP diagram of **6** ([Os(*p*-cymene)(*m*-CH_2NH_2)-Cl]PF_6) depicted with thermal ellipsoids at the 30% probability level. The counteranion and most of the hydrogens have been omitted for clarity. Selected bond distances (Å) and bond angles (deg): Os(1)−C(1), 2.07(1); Os(1)−N(3), 2.137(9); Os(1)−Cl(1), 2.422(3); Os(1)−C(12), 2.163(7); Os(1)−C(15), 2.201(6); C-(1)−Os(1)−N(3), 91.1(4); C(1)−Os(1)−Cl(1), 87.5(3); Cl-(1)−Os(1)−N(3), 80.0(3).

Experimental Section

Synthesis. All of the preparations and manipulations, except where otherwise stated, were carried out under a nitrogen or argon atmosphere using standard Schlenk-line and glovebox techniques. Dry and oxygen-free solvents were always used. The syntheses of [1-(2-(aminomethyl)phenyl)-3-methylimidazol-2-ylidene]chloro(η^6-*p*-cymene)ruthenium(II) hexafluorophosphate (**1**) and bis[1-(2-(aminomethyl)phenyl)-3-methylimidazol-2-ylidene]nickel(II) hexafluorophosphate (**5**) have been reported previously.[38] The synthesis of $[Os(p\text{-cymene})Cl_2]_2$[59,60] was reported in the literature. All other reagents and solvents were purchased from commercial sources and were used as received. Deuterated solvents were purchased from Cambridge

(63) Faller, J. W.; Lavoie, A. R. *Org. Lett.* **2001**, *3*, 3703–3706.

(64) (a) Flood, T. C.; Lim, J. K.; Deming, M. A.; Keung, W. *Organometallics* **2000**, *19*, 1166–1174. (b) Holland, A. W.; Bergman, R. G. *J. Am. Chem. Soc.* **2002**, *124*, 14684–14695. (c) Clarkson, A. J.; Buckingham, D. A.; Rogers, A. J.; Blackman, A. G.; Clark, C. R. *Inorg. Chem.* **2000**, *39*, 4769–4775.

Scheme 7. Proposed Mechanism for the H_2-Hydrogenation of Ketones Catalyzed by Complex 1 and Base

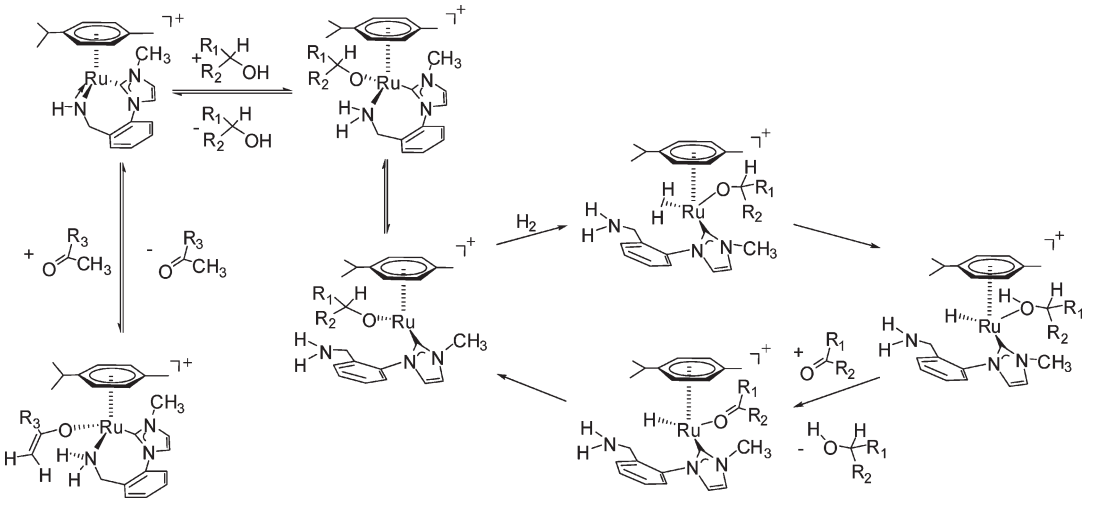

Isotope Laboratories and Sigma Aldrich and degassed and dried over activated molecular sieves prior to use. NMR spectra were recorded on a Varian 400 spectrometer operating at 400 MHz for ^{1}H, 100 MHz for ^{13}C, and 376 MHz for ^{19}F. The ^{1}H and ^{13}C{^{1}H} NMR spectra were measured relative to partially deuterated solvent peaks but are reported relative to tetramethylsilane (TMS). All ^{19}F chemical shifts were measured relative to trichlorofluoromethane as an external reference. Elemental analyses were performed at the Department of Chemistry, University of Toronto, on a Perkin-Elmer 2400 CHN elemental analyzer. Single-crystal X-ray diffraction data were collected using a Nonius Kappa-CCD diffractometer with Mo Kα radiation (λ = 0.710 73 Å). The CCD data were integrated and scaled using the Denzo-SMN package. The structures were solved and refined using SHELXTL V6.1. Refinement was by full-matrix least squares on F^2 using all data. Details are given in Table 5.

Synthesis of [1-(2-(Aminomethyl)phenyl)-3-methylimidazol-2-ylidene]hydrido(η^6-*p*-cymene)ruthenium(II) Hexafluorophosphate ([Ru(*p*-cymene)(*m*-CH_2NH_2)H]PF_6, 2). A Schlenk flask was charged with **1** (50 mg, 0.083 mmol) in 2-propanol solution (14 mL). The solution was warmed to 50 °C under an argon atmosphere. A solution of sodium 2-propoxide (20 mg, 0.24 mmol) in 2-propanol (6 mL) was added to this stirred solution over the course of 0.5 h, whereupon the color of the reaction mixture turned from yellow to deep red and then to brown. The solution was stirred for a further 3 h. After the reaction had gone to completion, the solvent was removed under vacuum. The solid residue was extracted with tetrahydrofuran (THF, 4 mL) and filtered through a pad of Celite. The addition of pentane (16 mL) to the THF solution yielded a brown precipitate, which was collected and dried in vacuo. Yield: 27 mg, 57%. Crystals suitable for an X-ray diffraction study were obtained as a THF solvate by slow diffusion of pentane into a saturated solution of **2** in tetrahydrofuran under a nitrogen atmosphere. ^{1}H NMR (CD_3CN, δ): 7.56 (m, 3-CH and 4-CH of Ph, 2H), 7.46 (m, 5-CH of Ph, 1H), 7.39 (d, J_{HH} = 7.34 Hz, 6-CH of Ph, 1H), 7.33 (d, J_{HH} = 1.72 Hz, 5-CH of imid, 1H), 7.21 (d, J_{HH} = 1.72, 4-CH of imid, 1H), 5.06 (d, J_{HH} = 5.65 Hz, 2-Ar-CH of *p*-cymene, 1H), 5.02 (d, J_{HH} = 5.92 Hz, 6-Ar-CH of *p*-cymene, 1H), 4.82 (d, J_{HH} = 5.92 Hz, 5-Ar-CH of *p*-cymene, 1H), 4.40 (d, J_{HH} = 5.65 Hz, 3-Ar-CH of *p*-cymene, 1H), 3.68 (m, CH_2, 1H), 3.61 (s, CH_3, 3H), 3.40 (m, br, NH_2, 2H), 2.64 (dt, J_{HH} = 3.66, 12.17 Hz, CH_2, 1H), 2.40 (sept, J_{HH} = 6.80 Hz, CH of $(CH_3)_2CH$ of *p*-cymene, 1H), 1.52 (s, CH_3 of *p*-cymene, 3H), 1.21 (d, J_{HH} = 6.80 Hz, CH_3 of $(CH_3)_2CH$ of *p*-cymene, 3H), 1.14 (d, J_{HH} = 6.80 Hz, CH_3 of $(CH_3)_2CH$ of *p*-cymene, 3H), −7.82 (s, Ru−H). ^{19}F NMR (CD_3CN, δ): −72.9 (d, J_{PF} = 706 Hz). ^{13}C{^{1}H} NMR (CD_3CN, δ): 185.3 (Ru−$C_{carbene}$), 141.4 (C_{Ph}), 134.0 (C_{Ph}), 132.2 (C_{Ph}), 130.5 (C_{Ph}), 129.3 (C_{Ph}), 126.6 (C_{Ph}), 124.3 ($C_{imid.}$), 123.5 ($C_{imid.}$), 108.7 ($C_{Ar\text{-}p\text{-}cymene}$), 105.1 ($C_{Ar\text{-}p\text{-}cymene}$), 88.9 ($C_{Ar\text{-}p\text{-}cymene}$), 85.6 ($C_{Ar\text{-}p\text{-}cymene}$), 81.3 ($C_{Ar\text{-}p\text{-}cymene}$), 80.9 ($C_{Ar\text{-}p\text{-}cymene}$), 47.4 ($CH_2$), 39.8 ($CH_3$), 32.4 (CH of $(CH_3)_2CH$ of *p*-cymene), 24.1 (CH_3 of $(CH_3)_2CH$ of *p*-cymene), 23.9 (CH_3 of $(CH_3)_2CH$ of *p*-cymene), 19.1 (CH_3 of *p*-cymene). MS (ESI, methanol/water; *m*/*z*): 424.1 $[M]^+$. Attempts at elemental analyses failed to give an acceptable carbon content, while hydrogen and nitrogen contents are in the acceptable range. Typical results are as follows. Anal. Calcd for $C_{21}H_{28}F_6N_3PRu$: C, 44.37; H, 4.96; N, 7.39. Found: C, 42.91; H, 4.80; N, 7.34.

Synthesis of [1-(2-(Aminomethyl)phenyl)-3-methylimidazol-2-ylidene]chloro(η^6-*p*-cymene)osmium(II) Hexafluorophosphate ([Os(*p*-cymene)(*m*-CH_2NH_2)Cl]PF_6, 6). A Schlenk flask was charged with **5** (46 mg, 0.064 mmol) and the $[Os(p\text{-cymene})Cl_2]_2$ dimer (50 mg, 0.063 mmol). Dry acetonitrile (8 mL) was added to the reaction mixture, and it was refluxed under an argon atmosphere for 2.5 h to give a green solution. The solvent was then evacuated. The residue was extracted with THF (4 mL) and filtered through a pad of Celite. The volume of solvent was reduced (2 mL), and addition of diethyl ether (12 mL) to the THF solution yielded a pale yellow precipitate which was collected and dried in vacuo. Yield: 81 mg, 93%. Crystals suitable for an X-ray diffraction study were obtained by slow diffusion of diethyl ether into a saturated solution of **6** in a 1/1 acetonitrile/methanol mixture under a nitrogen atmosphere. ^{1}H NMR (CD_2Cl_2, δ): 7.70 (m, 3-CH of Ph, 1H), 7.59 (m, 4-CH and 5-CH of Ph, 2H), 7.41 (m, 6-CH of Ph, 1H), 7.24 (d, J_{HH} = 1.95 Hz, 5-CH of imid, 1H), 7.22 (d, J_{HH} = 1.95, 4-CH of imid, 1H), 5.88 (m, br, NH_2, 2H), 5.58 (d, J_{HH} = 5.44 Hz, 2-Ar-CH of *p*-cymene, 1H), 5.51 (d, J_{HH} = 5.51 Hz, 6-Ar-CH of *p*-cymene, 1H), 5.30 (d, J_{HH} = 5.51 Hz, 5-Ar-CH of *p*-cymene, 1H), 4.98 (d, J_{HH} = 5.44 Hz, 3-Ar-CH of *p*-cymene, 1H), 4.21 (m, CH_2, 1H), 4.03 (s, CH_3, 3H), 3.15 (dt, J_{HH} = 2.54, 12.28 Hz, CH_2, 1H), 2.48 (sept, J_{HH} = 6.88 Hz, CH of $(CH_3)_2CH$ of *p*-cymene, 1H), 1.77 (s, CH_3 of *p*-cymene, 3H), 1.14 (d, J_{HH} = 6.91 Hz, CH_3 of $(CH_3)_2CH$ of *p*-cymene, 3H), 1.07 (d, J_{HH} = 6.91 Hz, CH_3 of $(CH_3)_2CH$ of *p*-cymene, 3H). ^{19}F NMR (CD_2Cl_2, δ): −72.0 (d, J_{PF} = 712 Hz). ^{13}C{^{1}H} NMR (CD_2Cl_2, δ): 159.4 (Os−$C_{carbene}$), 138.9 (C_{Ph}), 132.8 (C_{Ph}), 131.0 (C_{Ph}), 130.5 (C_{Ph}), 130.0 (C_{Ph}), 125.6 ($C_{imid.}$), 124.9 (C_{Ph}), 123.5 ($C_{imid.}$), 102.8 ($C_{Ar\text{-}p\text{-}cymene}$), 92.5 ($C_{Ar\text{-}p\text{-}cymene}$), 78.2 ($C_{Ar\text{-}p\text{-}cymene}$), 76.9 ($C_{Ar\text{-}p\text{-}cymene}$), 75.6 ($C_{Ar\text{-}p\text{-}cymene}$), 73.1 ($C_{Ar\text{-}p\text{-}cymene}$), 47.7 ($CH_2$), 39.8 ($CH_3$), 31.0 (CH of $(CH_3)_2CH$ of *p*-cymene), 23.9 (CH_3 of *p*-cymene), 21.2, (CH_3 of $(CH_3)_2CH$ of *p*-cymene), 18.7 (CH_3 of $(CH_3)_2CH$ of *p*-cymene). MS (ESI, methanol/

water; *m*/*z*): 548.2 $[M]^+$. HRMS (ESI, methanol/water; *m*/*z*): calcd for $C_{21}H_{27}N_3ClOs^+$ $[M]^+$ 548.1502, found 548.1463. Anal. Calcd for $C_{21}H_{27}ClF_6N_3OsP$: C, 36.44; H, 3.93; N, 6.07. Found: C, 37.04; H, 3.44; N, 5.51.

Catalysis. Oxygen-free tetrahydrofuran (THF) used for all of the catalytic runs was stirred over sodium for 2−3 days under argon and freshly distilled from sodium benzophenone ketyl prior to use. Acetophenone was vacuum-distilled over phosphorus pentoxide (P_2O_5) and stored under nitrogen prior to use. All of the other substrates were vacuum-distilled, dried over activated molecular sieves, and stored under nitrogen prior to use. All of the hydrogenation reactions were performed at constant pressure using a stainless steel 50 mL Parr hydrogenation reactor. The temperature was maintained at 50 °C using a constant-temperature water bath. The reactor was flushed several times with hydrogen gas at 2−4 bar prior to the addition of catalyst/substrate and base solutions.

In a typical run (Table 2, entry 2), the catalyst **1** (3 mg, 5.0 μmol), benzophenone (181 mg, 0.99 mmol), and potassium *tert*-butoxide (5 mg, 0.044 mmol) were dissolved in THF (4 and 2 mL, respectively) under a nitrogen atmosphere. The catalyst/substrate and base solutions were taken up by means of two separate syringes and needles in a glovebox. The needles were stoppered, and the syringes were taken to the reactor. The solutions were then injected into the reactor against a flow of hydrogen gas. The hydrogen gas was adjusted to the desired pressure. Small aliquots of the reaction mixture were quickly withdrawn with a syringe and needle under a flow of hydrogen at timed intervals by venting the Parr reactor at reduced pressure. Alternatively, small aliquots of the reaction mixture were sampled from a stainless steel sampling dip tube attached to a modified Parr reactor. The dip tube was 30 cm in length with an inner diameter of 0.01 in., and a swing valve was attached to the end of the sampling tube. Other technical details were previously reported.[18] Two small aliquots of samples were thereby withdrawn quickly at timed intervals by opening the swing valve, and the first two aliquots were discarded. All samples for gas chromatography (GC) analyses were diluted to a total volume of approximately 0.50 mL using oxygenated THF.

A Perkin−Elmer Clarus 400 chromatograph equipped with a chiral column (CP chirasil-Dex CB 25 m × 2.5 mm) with an autosampling capability was used for GC analyses. Hydrogen was used as a mobile phase at a column pressure of 5 psi with a split flow rate of 50 mL/min. The injector temperature was 250 °C, and the FID temperature was 275 °C. The oven temperature and the retention times (t_R, t_p, /min) for all the substrates and alcohol products are given in the Supporting Information (Table S7). All of the conversions were reported as an average of two GC runs. The reported conversions were reproducible.

Kinetics. A standard solution of the catalyst **1** (1.66 mM) was prepared by dissolving the complex (25 mg) in THF (25 mL). Reaction mixtures were then prepared in THF by dispensing the required amount of the catalyst and weighed amounts of acetophenone, phenylethanol, and potassium *tert*-butoxide (or a standard solution of potassium *tert*-butoxide (17.8 mM) in THF for base-dependent studies) and diluted to a total volume of 6 mL. The hydrogenation reaction and sampling techniques were described as above in order to obtain at least five data points including the origin (time 0 min) at below 40% conversion to the product alcohol. The tabulated results of initial rates with varying concentrations of catalyst, acetophenone, hydrogen, and potassium *tert*-butoxide are given in Table 3 and in the Supporting Information (Tables S1−S3). All of the conversions were reported as an average of at least two GC runs. The reported conversions were reproducible.

Kinetic Isotope Effect Studies. D_2 (99.8% D) gas and acetophenone-β,β,β-d_3 (99% D) were purchased from Cambridge Isotope Laboratories. Acetophenone-d_3 was vacuum-distilled, dried over activated molecular sieves, and stored under nitrogen prior to use. D_2 gas was used as received without further purification. For experiments using deuterium gas, the modified Parr reactor with a stainless steel sampling dip tube was used. The reactor was degassed by evacuation for 10 min, followed by refilling with 2−4 bar of deuterium gas. This was repeated three times. The reaction mixtures were then injected into the reactor against a flow of deuterium gas, and the gas pressure was adjusted to 8 bar. The tabulated results of the initial rates with varying concentrations of acetophenone are given in the Supporting Information (Tables S4−S6). Experiments using acetophenone-d_3 were conducted similarly to the kinetic studies described above.

Computational Details. All density functional theory (DFT) calculations were performed using the Gaussian03 package[65] with the restricted hybrid mPW1PW91 functional.[66] Ruthenium was treated with the SDD[67] basis set to include relativistic effects and an effective core potential, and other heteroatoms were treated with the double-ζ basis set 6-31++G**, which includes diffuse functionals and additional p orbitals on hydrogen as well as additional d orbitals on carbon, nitrogen, and oxygen. All geometry optimizations were conducted in the gas phase; these were followed by full vibrational analyses at 1 atm and 298 K. Reported energies were corrected from zero-point energies but uncorrected for translations and rotations. The QST3 method was used to locate transition states. All transition states reported were found to have a single imaginary frequency. The calculated atomic polar tensor (APT) charges were used to reflect more accurately the charge distribution on each atom under the derivative of dipole moments with respect to an applied external electric field.[68]

Acknowledgment. The NSERC of Canada is thanked for a Discovery Grant to R.H.M. NSERC Canada and the Ministry of Education of Ontario are thanked for graduate scholarships to W.W.N.O.

Supporting Information Available: CIF files giving X-ray structural data for complexes **2** and **6**, text, tables, and figures giving details for catalysis and tabulated results for kinetic data, experimental procedures, and characterization data of complex **4**, Cartesian coordinates, energies for all of the computed structures, and the complete citation for reference 65, and AVI files giving animations for the computed transition states. This material is available free of charge via the Internet at http://pubs.acs.org.

(65) Frisch, M., et al. *Gaussian 03, Revision C.02*; Gaussian Inc., Wallingford, CT, 2004.
(66) (a) Adamo, C.; Barone, V. *J. Chem. Phys.* **1998**, *108*, 664–675. (b) Burke, K.; Perdew, J. P.; Wang, Y. *Electronic Density Functional Theory: Recent Progress and New Directions*; Plenum: New York, 1997.
(67) Leininger, T.; Nicklass, A.; Stoll, H.; Dolg, M.; Schwerdtfeger, P. *J. Chem. Phys.* **1996**, *105*, 1052–1059.
(68) Cioslowski, J. *J. Am. Chem. Soc.* **1989**, *111*, 8333–8336.